

PUBLISHED BY

INTECH

open science | open minds

World's largest Science,
Technology & Medicine
Open Access book publisher



2800+
OPEN ACCESS BOOKS



97,000+
INTERNATIONAL
AUTHORS AND EDITORS



90+ MILLION
DOWNLOADS



BOOKS
DELIVERED TO
151 COUNTRIES

AUTHORS AMONG
TOP 1%
MOST CITED SCIENTIST



12.2%
AUTHORS AND EDITORS
FROM TOP 500 UNIVERSITIES



Selection of our books indexed in the
Book Citation Index in Web of Science™
Core Collection (BKCI)

Chapter from the book *Recent Advances in Multi Robot Systems*

Downloaded from:

http://www.intechopen.com/books/recent_advances_in_multi_robot_systems

Interested in publishing with InTechOpen?
Contact us at book.department@intechopen.com

Randomized Robot Trophallaxis

Trung Dung Ngo and Henrik Schiøler (equal)

Aalborg University

Denmark

1. Introduction

Energy is the critical resource of most living mechanisms. Recent research in robotics has been mostly considered in behavioural autonomy rather than in energy autonomy. This chapter presents our study in “randomized robot trophallaxis”. The chapter consists of three main parts: modeling, simulation, and implementation.

In the first section, we model energy trophallaxis in multi-robot system through probabilistic modelling. Deterministic modelling of large groups of interacting mobile robots leads to highly complex nonlinear hybrid models, likely to be highly sensitive to pre-conditions, i.e. chaotic. Thus, any imprecision in pre-conditions would turn results from such a model useless even for moderate time horizons. However, chaotic systems often exhibit smooth ergodic properties, i.e. time averages have limit values independent of initial conditions and only smoothly dependent on model parameters, etc. Randomness and ergodic properties may exist naturally in such systems or even be intentionally enforced by introducing inherent uncertainty/randomization into the behaviour of individual robots in order to prevent non productive cyclic behaviour such as deadlock or livelocks. Ergodic properties and randomness calls for probabilistic modelling. We propose a combined probabilistic model covering energy exchange between robots, energy consumption in individual robots, charging at predefined charging stations and finally random mobility, where the latter comes in the shape of highly versatile Markovian mobility model. Stationary results furnish overall system performability analysis, such as the impact of individual behaviour on overall system survivability. The section presents the proposed model and comprises central parts of model development as well as illustrative numerical results.

In the second section, we simulate aspects of energy autonomy inspired by natural phenomena of animal behaviour. Trophallaxis is a natural phenomenon, biologically observed from social insects or vertebrate animals, to exchange food between colony members. This section describes the concept, “Randomized Robot Trophallaxis”, based on a group of autonomous mobile robots with capabilities of self-refueling energy and self-sharing energy. We firstly clarify the concept “Randomized Robot Trophallaxis” by given examples of natural animal societies. Secondly, we examine the concept by simulation results in order to point out considerable advantages of trophallactic features when deploying multiple mobile robots. The section is concluded with discussion of “randomization” and its appearances in multi-robot system.

In the third section, we mainly present hardware implementation of our mobile robots capable of performing not only self-refueling energy but also self-sharing energy. We describe the mechanical and electrical design of a mobile robot, called the CISSbot¹. The robots are designed towards truly autonomous robots in large populations through energy trophallaxis. Unlike present mobile robots, the CISSbots are energetically autonomous robots because they are able to not only autonomously refuel energy by picking batteries up at a charging station, but also share energy by exchanging batteries to other robots. The CISSbots basically consist of their own processing power, sensors, and actuators. However, to achieve the capability of battery exchange, the CISSbots need a special design of battery exchange mechanism. In this section, we present the realization of the design, both the mechanics and the electronics of the CISSbot. Details on battery exchange technique and power management are clarified. Finally, the section issues an outline of our future work on the CISSbots.

2. A Probabilistic Model of Randomized Robot Trophallaxis

2.1 An Introduction to Probabilistic Modelling

Various mathematical modelling paradigms exist for dynamical systems, which all aim to provide system predictability, i.e. answer questions regarding future state of the system evolving from some initial state or set of initial states. The appropriate model paradigm depends highly on the nature of the questions to be answered, i.e. the scope of required information as well as the form of the answer provided by the model. In the present case, we ask for distribution of energy resources throughout the population of mobile robots as well as the survival state of the population, i.e. how many robots have survived energy starvation over a certain time frame. Of particular interest is the impact, that individual robot behaviour may have on energy distribution and survival.

Any such model should include all aspects of robot behaviour suspected to impact population state. Here we suggest: mobility, energy sharing policy and recharging as well as energy consumption.

Deterministic models appear as differential equations, as discrete state transition systems or combinations of the two former when hybrid modelling is applied. Common to deterministic models is their ability to provide exact answers to exactly formulated questions. That is, when all pre-conditions are exactly stated the future may be exactly predicted. When pre-conditions are only partly known, non-deterministic modelling in the shape of differential inclusions or non-deterministic state transition systems, may be applied. The precision of non-deterministic models follows the precision by which pre-conditions are given.

From a deterministic modelling perspective, large groups of interacting mobile robots correspond to a highly complex nonlinear hybrid model, which is likely to be highly sensitive to pre-conditions, i.e. chaotic. Thus, any imprecision in pre-conditions would turn results from such a model useless even for moderate time horizons. On the other hand chaotic systems like large interacting robot populations are likely to possess so called *mixing* properties. Mixing implies, that from partly known pre-conditions, almost any future development is possible even within moderate time horizons. Thus precision of answers

¹ CISSbot is abbreviated from our center in Danish: Center for Indlejrede Software Systemer (CISS).
<http://www.ciss.dk>

from non-deterministic models of mixing systems rapidly deteriorates with time. Chaotic systems with mixing properties often exhibit smooth *ergodic* properties, i.e. time averages have limit value independent of initial conditions and only smoothly dependent on model parameters. In other words such systems exhibit predictable statistics. Mixing or ergodic properties may be enforced onto the system by introducing uncertainty/randomization into the behaviour of individual robots. This may prevent the overall system from getting stuck in non productive cyclic behaviour such as deadlock or live locks. As an example randomization is used for wireless access protocols and suggested for the so called *leader election* problem.

Based on the previous arguments we suggest a probabilistic model for trophallaxis among mobile robots including mobility, energy sharing policy and recharging as well as energy consumption. Such a model may serve as the basis for long term stochastic simulation, in which case ergodic properties become critical w.r.t. the meaningfulness of the obtained results. On the other hand, the model may be mathematically tractable, allowing for direct numerical assessment of the coupling between individual behavioural parameters and overall system state. Such a model is presented below.

2.2 Modelling

The developed model aims to combine the effects of all the influential mechanisms associated to trophallaxis in mobile robot populations: mobility, resource sharing, charging and resource consumption. Initially separate models are developed for each of the above effects, which are then assumed additive and conditionally independent given instant system state. System state is defined to be the position $x_i(t)$ of every robot i , its velocity $v_i(t)$ as well as its energy resource $b_i(t)$.

Since we aim for a probabilistic model, exact values of x_i , v_i and b_i are not tracked. Instead the developed model follows the evolution of the distribution of these random variables and in particular the distribution obtained in stationarity. Non parametric equations are developed for distributions of x_i and v_i , whereas the distribution for b_i is described in terms of 1 st. and 2 nd. moments. To ease exposition, velocities are assumed to take values within a discrete set.

Each separate model for resource sharing, charging and consumption are given as integro-differential equations governing the time evolution of the conditional expectation $b_i(t, x, v) = E(b_i(t)|x_i(t) = x, v_i(t) = v)$ of the resource $b_i(t)$ carried by robot i , given it is located at x at time t , with velocity v . Likewise a second moment model is developed for the time evolution of the conditional variance $V_i(t, x, v) = VAR(b_i(t)|x_i(t) = x, v_i(t) = v)$.

2.2.1 Mobility

Robot populations may be distributed randomly over some domain D , or they may be deployed according to some predefined plan. Additionally robots may be stationary or mobile, e.g. a subset of robots may be assigned highly stationary tasks, whereas a majority of units would be mobile.

A model of robot distribution should account for both deterministic deployment and random distribution. We assign to each robot i the time dependent probability measure L_i of location, i.e. $L_i(A, t)$ expresses the probability that node i is located within the subset A of D , at time t . Adding up for the entire set of nodes yields the additive positive measure L , i.e.

$$L(A, t) = \sum_i L_i(A, t) \quad (1)$$

where $L(A, t)$ expresses the expected number of robots within A at time t . Joint location and velocity measure is assumed to be expressed as

$$L_i(A \times W, t) = \int_A L_i(W|x, t) f_L^i(x, t) dx \quad (2)$$

i.e. position distribution is described by a density f_L^i , whereas velocity has a general conditional distribution $L_i(W|x)$. The notation L_i is consistently used for kinetic state (position and velocity) distribution of robot i . The corresponding argument list indicates the specific perspective in question.

Mobility affects resource distribution in two ways; it changes robot location distribution over time and secondly it changes the conditional resource distribution over time. The former effect is considered in this section whereas the latter is presented in the next section based on the stationary location distribution obtained in this section. Several mobility models exist, including deterministic as well as random movement. Among others we find the *Random waypoint* [Bettstetter et al, 2004], *Random direction* and *Random trip* [Le Boudec et al, 2005] an overview is presented in [Camp et al, 2002]. In this work we consider mobility models both suited for probabilistic modelling of which a special case is Brownian motion [Øksendal et al, 2003]. Brownian motion is characterized by its lack of velocity persistence, i.e. units move without memory of previous direction and speed. A more elaborate model is presented subsequently, which includes velocity persistence.

2.2.2 Less Drunk Model

The Less Drunk Model (LDM) is as Brownian motion a Markovian mobility model, where velocity remains constant between instants $\dots, t_{-1}, t_0, t_1, \dots$ of velocity change. Time intervals of constant velocity have random exponentially distributed length, where the intensity parameter λ may depend on position, velocity and time. At an instant t_n of velocity change, a future velocity is selected randomly and independently from a probability distribution L_Q assumed to depend on position.

So equipped we may deduce the following location distribution dynamics

$$\begin{aligned} & \frac{d}{dt} (L_i(W|x, t) \cdot f_L^i(x, t)) \\ &= \lambda(x) (L_Q(W, x) - L_i(W|x, t)) f_L^i(x, t) \\ & - \int_W \langle v, D_x [L_i(dv|\cdot, \cdot) f_L^i](x, t) \rangle \end{aligned} \quad (3)$$

where $\langle \cdot, \cdot \rangle$ denotes inner product. The second term generalises continuous and discrete parts of L_i , i.e.

$$\begin{aligned} & \int_W \langle v, D_x [L_i(dv|\cdot, \cdot) f_L^i](x, t) \rangle \\ &= \int_W \langle v, D_x [f_i(dv|\cdot, \cdot) f_L^i](x, t) \rangle \\ &+ \sum_{v_j \in W} \langle v, D_x [L_i(\{v_j\}|\cdot, \cdot) f_L^i](x, t) \rangle \end{aligned}$$

As an example, L_Q may for all x concentrate probability on a discrete set of velocities $\{v_j\}$. Letting $W = \{v_j\}$ gives

$$\begin{aligned} & \frac{d}{dt} (L_i(\{v_j\}|x, t) \cdot f_L^i(x, t)) \\ &= \lambda(x)(L_Q(\{v_j\}, x) - L_i(\{v_j\}|x, t))f_L^i(x, t) \\ &- \langle v_j, D_x[L_i(\{v_j\}|\cdot, \cdot)f_L^i](x, t) \rangle \end{aligned} \quad (4)$$

Confinement of motion to a Consider a one-dimensional example, where velocities assume values 1 and -1 .

$$\begin{aligned} L_Q(\{1\}, x) &= 1/2 \text{ for } -1 \leq x \leq 1 \\ &= 0 \text{ for } x > 1 \\ &= 1 \text{ for } x < -1 \\ L_Q(\{-1\}, x) &= 1/2 \text{ for } -1 \leq x \leq 1 \\ &= 0 \text{ for } x < -1 \\ &= 1 \text{ for } x > 1 \end{aligned} \quad (5)$$

for a constant value $\lambda(x) = \lambda$ for x outside $[-1, 1]$ (4) possesses the following particular stationary solution

$$\begin{aligned} L_i(\{-1\}|x, t) f_L^i(x, t) &= L_i(\{-1\}|x, t) f_L^i(x, t) \\ &= C_0 \text{ for } x \in [-1, 1] \\ &= C_0 \exp(\lambda(x-1)) \text{ for } x \in (-\infty, -1) \\ &= C_0 \exp(\lambda(1-x)) \text{ for } x \in (1, \infty) \end{aligned} \quad (6)$$

where $C_0 = 1/4(1 + 1/\lambda)$ is found from normalization. Stationary solutions for various λ values are shown in figure (1). For large λ , C_0 is approximately 1/4 and $f_L^i(x, t) = 1/2$ inside D .

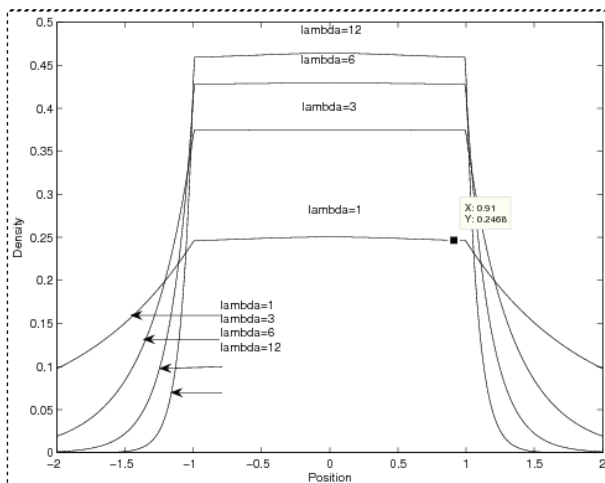


Figure 1. Stationary location densities for various λ -values

2.2.3 Mobility Impact on Energy Distribution

Consider a small sub domain A at times t and $t + \delta$. Not considering exchange nor consumption, the amount of energy resources carried by robot i in A at time $t + \delta$ is identical to the amount of resources moving (along with robot i) into $A \times \{v_j\}$ during $[t, t + \delta]$. The expected energy resource $E_{A \times \{v_j\}}(t + \delta)$ in $A \times \{v_j\}$ at time $t + \delta$, is expressed through the conditional resource given position and velocity $b_i(t, x, v)$, i.e.

$$E_{A \times \{v_j\}}(t + \delta) = \int_A b_i(t + \delta, x, v_j) L_i(\{v_j\} | x) f_L^i(x) dx \quad (2.3.1)$$

whereas the amount carried into $A \times W$ by i is found by conditioning on position and velocity x' and v' at time t and marginalizing, i.e.

$$\begin{aligned} & E_{A \times \{v_j\}}(t + \delta) \\ & + (1 - \lambda \delta) \int_A b_i(t, x - v_j \delta, v_j) f_L^i(x - v_j \delta) L_i(\{v_j\} | x - v_j \delta) dx \\ & + \lambda \delta \int_A L_Q(\{v_j\}, x) \sum_k b_i(t, x - v_k \delta, v_k) f_L^i(x - v_k \delta) L_i(v_k | x - v_k \delta) dx \end{aligned} \quad (8)$$

Equating expressions (7) and (8) for every subset A and differentiating w.r.t. δ , we may show that $b_i(t, x, v)$ fulfills

$$\begin{aligned} & f_L^i(x) L_i(\{v_j\} | x) \frac{d}{dt} b_i(t, x, v_j) \\ & = - \langle v_j, D_x [b_i f_L^i L_i](t, x, v_j) \rangle \\ & + \lambda (L_Q(\{v_j\}, x) b_i(t, x) - L_i(\{v_j\} | x) b_i(t, x, v_j)) f_L^i(x) \end{aligned} \quad (9)$$

where

$$b_i(t, x) = \sum_k b_i(t, x, v_k) L_i(\{v_k\} | x) \quad (10)$$

Equivalent results can be found for then conditional second moment $b2_i$

$$\begin{aligned} & f_L^i(x) L_i(\{v_j\} | x) \frac{d}{dt} b2_i(t, x, v_j) \\ & = - \langle v_j, D_x [b2_i f_L^i L_i](t, x, v_j) \rangle \\ & + \lambda (L_Q(v_j, x) b2_i(t, x) - L_i(\{v_j\} | x) b2_i(t, x, v_j)) f_L^i(x) \end{aligned} \quad (11)$$

2.2.4 Numerical Example

We continue the numerical example from above and extend it with expressions and results for energy distribution. We assume the stationary solution (6) for $f_L^i L_i$ for each robot i . Likewise we assume λ to be high outside D and thereby neglecting movement outside D . Thus we have $f_L^i L_i = 1/4$ inside D and zero outside. Likewise

$$\begin{aligned} & \langle v_j, D_x [b_i f_L^i L_i](t, x, v_j) \rangle = 1/4 \langle v_j, D_x [b_i](t, x, v_j) \rangle \\ & \langle v_j, D_x [b2_i f_L^i L_i](t, x, v_j) \rangle = 1/4 \langle v_j, D_x [b2_i](t, x, v_j) \rangle \end{aligned} \quad (12)$$

altogether we have from (9) and (11)

$$\begin{aligned}\frac{d}{dt} b_i(t, x, v_j) &= - \langle v_j, D_x[b_i](t, x, v_j) \rangle + \lambda (b_i(t, x) - b_i(t, x, v_j)) \\ \frac{d}{dt} b_{2i}(t, x, v_j) &= - \langle v_j, D_x[b_{2i}](t, x, v_j) \rangle + \lambda (b_{2i}(t, x) - b_{2i}(t, x, v_j))\end{aligned}\quad (13)$$

Inserting discrete velocities $\{1\}$ and $\{-1\}$ gives

$$\begin{aligned}\frac{d}{dt} b_i(t, x, -1) &= b'_i(t, x, -1) + \lambda/2(b_i(t, x, 1) - b_i(t, x, -1)) \\ \frac{d}{dt} b_i(t, x, 1) &= -b'_i(t, x, 1) + \lambda/2(b_i(t, x, -1) - b_i(t, x, 1)) \\ \frac{d}{dt} b_{2i}(t, x, -1) &= b'_{2i}(t, x, -1) + \lambda/2(b_{2i}(t, x, 1) - b_{2i}(t, x, -1)) \\ \frac{d}{dt} b_{2i}(t, x, 1) &= -b'_{2i}(t, x, 1) + \lambda/2(b_{2i}(t, x, -1) - b_{2i}(t, x, 1))\end{aligned}\quad (14)$$

revealing that, when mobility is studied in isolation, stationary solutions for expected battery resources as well as second moments are constant over D , which coheres well with intuition.

2.2.5 Energy Transfer

Energy exchange is in this work considered to be an unplanned epidemic process, i.e. transfer of energy between robots take place during accidental rendezvous. Epidemic propagation is previously studied in other contexts, such as disease spread [Medlock et al, 2003] and information spread [Schiøler et al, 2005],[Moreno et al, 2004]. All mobile units are assumed to move randomly in patterns generated by a Less Drunk mobility process as described above. When two robots come within a suitable (not too large) distance to each other, conditions promote energy exchange as illustrated in figure (2).

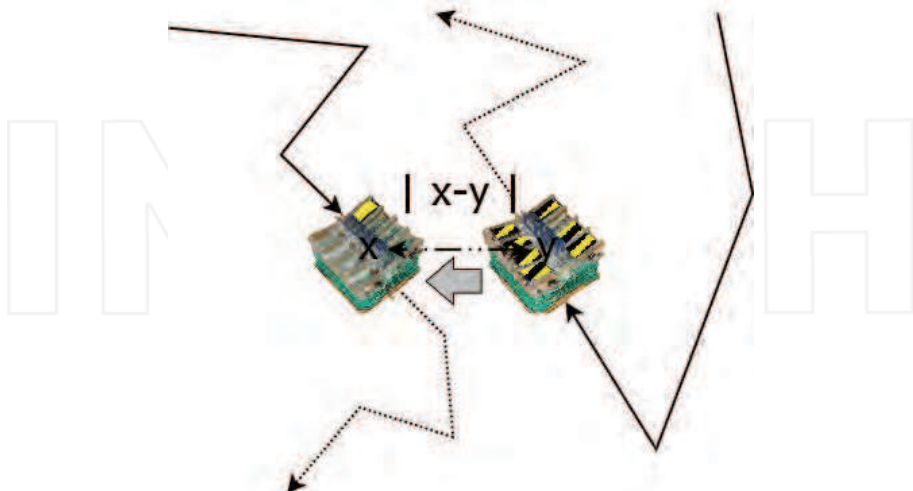


Figure 2. Two robots in accidental rendezvous, candidating for energy exchange

More precisely two robots i and j positioned at positions $x = x_i$ and $y = x_j$ respectively are assumed to engage in a battery exchange within the time interval $[t, t + dt]$ with a probability $\alpha dt K(x_i, x_j)$, where α is a rate parameter and K is a *neighbourhood kernel* modelling the dependence of relative/absolute positions on exchange probability. The decision to engage in battery exchange is taken randomly and represented by the random Boolean selector Ce_{ij} , where $P(Ce_{ij}) = \alpha dt K(x_i, x_j)$. At time t robots i and j mutually communicate remaining battery resources $b_i(t)$ and $b_j(t)$ respectively. The final choice of battery exchange is taken randomly and represented by the random Boolean selector Cf , where

$$P(Cf_{ij}) = C|b_i(t) - b_j(t)| \quad (15)$$

where C is chosen, so that $P(Cf) \leq 1$ always. If exchange is decided, a fixed size quantity Q is exchanged, where $Q = |Q| \operatorname{sign}(b_j(t) - b_i(t))$. Altogether the exchange dynamics for two robots can be written as

$$b_i(t + dt) = b_i(t) + Ce_{ij} Cf_{ij} |Q| \operatorname{sign}(b_j(t) - b_i(t)) \quad (16)$$

Potentially i may exchange batteries with every other robot j in the entire population, so the overall exchange dynamics can be written like

$$b_i(t + dt) = b_i(t) + \sum_{j \neq i} Ce_{ij} Cf_{ij} |Q| \operatorname{sign}(b_j(t) - b_i(t)) \quad (17)$$

When robot positions are unknown, a location measure L_i is associated to each robot i . Likewise we define $b_i(t, x, v)$ to be the conditional expectation of $b_i(t)$ given i is positioned at x with velocity v at time t . Thus from (16)

$$\begin{aligned} b_i(t + dt, x, v) &= b_i(t, x, v) + |Q| \sum_{j \neq i} E[Ce_{ij} Cf_{ij} \operatorname{sign}(b_j(t) - b_i(t))] \\ &= b_i(t, x, v) + |Q| C \alpha dt \sum_{j \neq i} E[K(x, x_j) |b_j(t) - b_i(t)| \operatorname{sign}(b_j(t) - b_i(t))] \\ &= b_i(t, x, v) + |Q| C \alpha dt \sum_j \int_D K(x, y) b_j(t, y) - b_i(t, x, v) L_j(dy) \end{aligned} \quad (18)$$

Where velocity is marginalized away in b_j , i.e.

$$b_j(t, y) = \int b_j(t, y, v) L_j(dv|x) \quad (19)$$

Adding location measures ($L = \sum_j L_j$), leads from (18) to

$$\begin{aligned} \frac{d}{dt} b_i(t, x, v) &= |Q| C \alpha \sum_j \int_D K(x, y) b_j(t, y) L_j(dy) \\ &\quad - |Q| C \alpha b_i(t, x, v) \int_D K(x, y) L(dy) \end{aligned} \quad (20)$$

and for the conditional second moment $b2_i(t, x, v)$ of $b_i(t)$ given position x and velocity v at time t .

$$\begin{aligned} \frac{d}{dt} b2_i(t, x, v) = & 2|Q|C\lambda (b_i(t, x, v) \sum_j \int_{\Omega} K(x, y) b_j(t, y) L_j(dy) - b2_i(t, x, v) \int_{\Omega} K(x, y) L(dy)) \\ & + |Q|C\lambda \sum_j \int_{\Omega} K(x, y) |b_j(t, y) - b_i(t, x, v)| L_j(dy) \end{aligned} \quad (21)$$

2.2.6 Charging Station

Charging stations may be considered as only robot units serving special objectives. Formally we define a robot i to be a charging station, when $i \in CS$, where CS is the index subset for charging stations.

Specific to charging stations is the fact, that batteries should never be received by these, and additionally that they may move according to a specific mobility patterns. With respect to the former exception we exclude from the model the resource level of charging stations and simply assume resource levels always to assume an upper bound, i.e. $b_i(t, x) = \bar{b} \forall t, x$. This excludes the possibility of battery units to be handed over to charging stations. Likewise it may be desirable to have separate control of the exchange rate from the charger. Thus we set the exchange rate parameter for the charger by $\alpha_C = r_C \alpha$, where r_C is a positive real typically > 1 .

Regarding mobility of charging stations, they may as a first suggestion be stationary at known locations. Location measure L_i for a charging station is in, this case, concentrated at a particular point x_C , i.e. $L_i(\{x_C\}) = 1$. Even for stationary charging stations, locations may be unknown, in which case locations are specified according to some a priori measure L_i . For non stationary charging stations some mobility model may be assumed and L_i may be time dependent converging to a stationary measure as for robot units.

2.2.7 Example

Continuing the above example we have for mobile units $L_j(A) = |A|/|D|$. Furthermore we assume $b_i(t, x, v) = b(t, x, v)$ for all mobile units i , whereas $L_i(A) = I_A(x_C)$ and $b_i(t, x, v) = \bar{b}$ for a single charging station located at a fixed position x_C . Assuming N robots equations (20) and (21) yield

$$\begin{aligned} \frac{d}{dt} b(t, x, v) & = |Q|C\alpha N/|D| \\ & \cdot \int_D K(x, y) \left(\frac{b(t, y, \{-1\}) + b(t, y, \{1\})}{2} - b(t, x, v) \right) dy \\ & + |Q|C\alpha r_C K(x, x_C) (\bar{b} - b(t, x, v)) \end{aligned} \quad (22)$$

and for the conditional second moment $b2(t, x, v)$

$$\begin{aligned}
& \frac{d}{dt} b2(t, x, v) = \\
& -2|Q|C\alpha b2(t, x, v)(N/|D| \int_D K(x, y)dy + r_C K(x, x_C)) \\
& + 2|Q|C\alpha 2b(t, x, v) \\
& \cdot (N/|D| \int_D K(x, y) \frac{b(t, y, \{-1\}) + b(t, y, \{1\})}{2} dy + r_C \bar{b} K(x, x_C)) \\
& + |Q|C\alpha \\
& \cdot (N/|D| \int_D K(x, y) |b_j(t, y) - b_i(t, x, v)| dy \\
& + r_C K(x, x_C) |\bar{b} - b_i(t, x, v)|)
\end{aligned} \tag{23}$$

2.2.8 Energy Consumption

Various models for energy consumption in mobile robotics are suggested in literature [Mei et al, 2006a, 2006b]. In this case choosing a suitable model involves a trade-off between precision and mathematical tractability. The rate of energy consumption may depend on various parts of the system state, i.e. on aspects of the state of the entire population as well as the state of the individual robot. Since robots may be equipped with energy preserving activity policies, their individual activity may depend on their remaining energy resources. Taking such behaviour into account may be achieved by letting consumption rate depend on remaining resources. In this case we suggest a Poisson modulated model, i.e.

$$b_i(t) = b_i(0) \cdot \exp^{-n}(-r/\gamma) \text{ for } t \in [t_n, t_{n+1}] \tag{24}$$

where $\{t_n\}$ is an increasing Poisson generated sequence of time instants, where remaining battery resources are discounted through multiplication by $\exp(-r/\gamma) < 1$ so that (2.8.1) exhibits an expected exponential consumption profile, i.e.

$$\begin{aligned}
& E(b_i(t)|x_i(t) = x, v_i(t) = v) = b_i(t, x, v) \\
& = b_i(0, x, v) \cdot \exp(-\gamma t(1 - \exp(-r/\gamma)))
\end{aligned} \tag{25}$$

which, for large values of γ can be approximated by

$$b_i(t, x, v) = b_i(0, x, v) \cdot \exp(-rt) \tag{26}$$

For our Poisson modulated consumption model (23), we may deduce

$$\begin{aligned}
& \frac{d}{dt} b_i(t, x, v) = \gamma (\exp(-r/\gamma) - 1) b_i(t, x, v) \\
& \frac{d}{dt} b2_i(t, x, v) = \gamma (\exp(-2r/\gamma) - 1) b2_i(t, x, v)
\end{aligned} \tag{27}$$

which for large values of γ can be approximated by

$$\begin{aligned}
& \frac{d}{dt} b_i(t, x, v) = -r b_i(t, x, v) \\
& \frac{d}{dt} b2_i(t, x, v) = -2r b2_i(t, x, v)
\end{aligned} \tag{28}$$

2.2.9 Complete Model

A complete model is presented which combines the effects of mobility, energy exchange and energy consumption. The developed model assumes the shape of integro-differential equations governing the time evolution of the conditional expectation $b_i(t, x, v)$ of the battery resource $b_i(t)$ of robot i given this robot is located at position x at time t , with velocity v . Likewise integro-differential equations for the conditional variance $b2_i(t, x, v) = E(b_i^2(t))$ are given. The model is developed for stationary location distributions.

All individual model parts (mobility, exchange, consumption) are developed from elementary dynamics giving $b_i(t + \delta)$ from $b_i(t)$ for an infinitesimal time step δ , i.e. $b_i(t + \delta) = b_i(t) + D_M(\delta)$, $b_i(t + \delta) = b_i(t) + D_E(\delta)$, $b_i(t + \delta) = b_i(t) + D_C(\delta)$, where D_M , D_E and D_C are random variables modelling randomized mobility, energy exchange and energy consumption respectively. Thus the complete integro-differential equation for conditional expectation is found as

$$\frac{d}{dt}(b_i(t, x, v)) = \frac{d}{d\delta}E[D_M(\delta)] + \frac{d}{d\delta}E[D_E(\delta)] + \frac{d}{d\delta}E[D_C(\delta)] \quad (29)$$

D_M , D_E and D_C are assumed independent, being continuous at $\delta = 0$ and having 1st. and 2nd. moments with finite non-zero 1st. derivatives at $\delta = 0$. This allows aggregation of separate model components for conditional 2nd. moments by addition i.e.

$$\frac{d}{dt}b2_i(t, x, v) = \frac{d}{d\delta}E[D_M^2(\delta)] + \frac{d}{d\delta}E[D_E^2(\delta)] + \frac{d}{d\delta}E[D_C^2(\delta)] \quad (30)$$

2.2.10 Example

The complete model is illustrated by examples combining the previous examples in this chapter. It is not possible to provide an overview of results for the entire parameter space, so therefore only a few illustrative examples are shown. Parameter settings for the provided examples are selected below to mimic a realistic situation. It is basically assumed that all robots inhabit a one-dimensional domain of operation $D = [-1, 1]$ and move with two possible speeds $\{-1, 1\}$. Thus crossing the entire domain without speed changes lasts 2 time units.

For the mobility parameter λ we assume robots to change velocity 10 times for each such 2 time units, i.e. $\lambda = 5$.

In order for an energy propagation mechanism to be worthwhile, a significant power loss should be associated with travelling from the peripheral of the domain of operation to the charger. Thus we assume, that a direct travel half way across D discounts the energy resources by 2/3, i.e. $\exp(-r) = 0.3$ or $r \approx 1$.

Regarding energy exchange, we normalize the charger resource by $\bar{b} = 1$ defining an upper bound for b_i . In accordance we set $C = 1$ and $Q = 1/10$, that is, the energy quantum exchanged is far lower than the upper bound for remaining resource. The neighbourhood kernel K is assumed to allow energy exchange within a fixed distance $d = 0.1$, i.e. $K(x, y) = I_{|x-y|<0.1}$. The charging process is assumed to be faster than the energy consumption process. Thus we set $\gamma < \alpha_C = 40$. The mutual robot exchange rate α is varied to illustrate its effect on energy distribution. A charger placed at a fixed location $x_C = 0$ serves $N = 50$ robots.

2.11 Survivability

Energy resources at each robot needs to be above a certain critical lower level L to maintain robot functionality. Below this level robots are no longer capable of moving, communicating or exchanging energy. Thus energy levels below L implies irreversible entrance to a *death* state. The suggested consumption model above prescribes consumption to take place at discrete moments $\{t_n\}$ in time, where energy resources are discounted by a factor $\exp(-r/\gamma)$. Every robot holding an energy level less than $L \exp(r/\gamma)$ is therefore a candidate for entering the death state at the next discrete consumption instant t_n . Since $\{t_n\}$ is assumed to be a homogeneous Poisson process with intensity γ the death rate associated to such a robot is γ . Likewise we may find the overall expected death rate ρ_D of the population by

$$\rho_D = P(b(t) \leq L \exp(r/\gamma)) N \gamma \quad (31)$$

Approximating the conditional stationary distribution of $b_i(t)$ by a normal distribution we get

$$\rho_D = \int_D \operatorname{erf}(L \exp(r/\gamma) \cdot \sigma_i(x, v) - b_i(x, v)) L_i(dv|x) f_i(x) dx N \gamma \quad (32)$$

where $\sigma_i = \sqrt{b_{2i} - b_i^2}$ is the conditional standard deviation and $\operatorname{erf}()$ is the error function. Figures (3) and (4) show stationary energy distributions for values of α 0.5 and 10. Corresponding death rate values are $\rho_D = 268$ and $\rho_D < 2E-16$, where the latter indicates a result below machine precision. Thus the effect of the mutual exchange rate is rather dramatic.

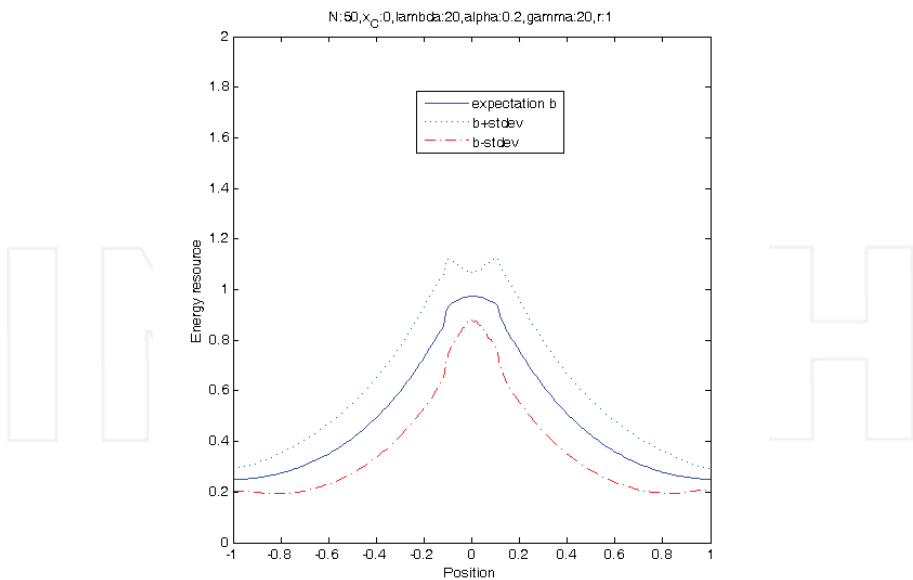


Figure 3. Energy distributions for low level of $\alpha = 0.2$

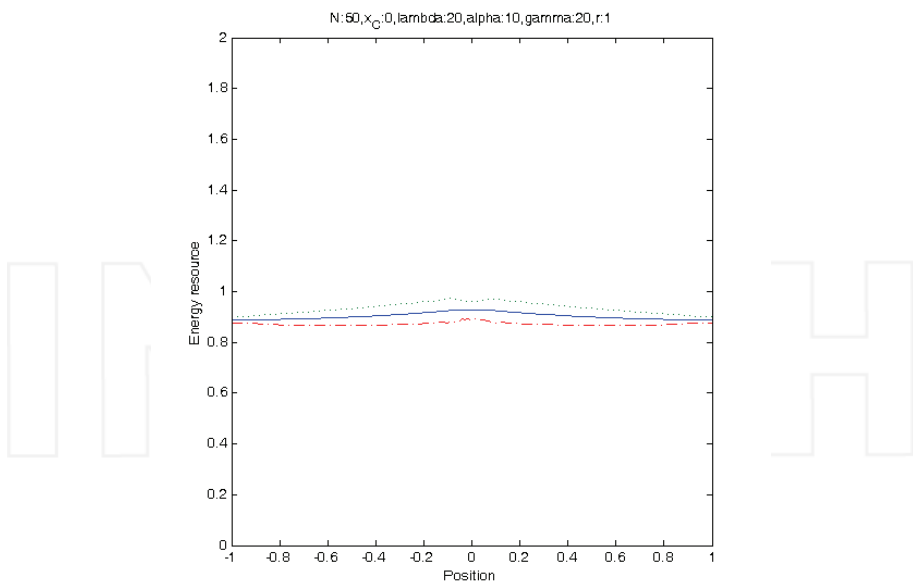


Figure 4. Energy distributions for high level of $\alpha = 10$

An increased mutual exchange rate increases the flow of energy away from the neighbourhood of the charger, which in turn allows more flow from the charger to its neighbourhood. Additionally, mutual exchange transports energy resources to the peripheral of D increasing survival far away from the charger. As seen from figures (3) and (4) mutual exchange levels energy resources among robots and in turn reduces variance and improves survival.

3. Biologically Inspired Robot Trophallaxis Simulation

3.1 An introduction to Biologically Inspired Robot Trophallaxis

The term “trophallaxis” is simply defined as mutual exchange of food between adults and larvae of certain social insects or between parents and offspring of vertebrate animals [Camazine, 1998]. In other words, trophallaxis is the regurgitation of food by one animal for the other in a colony. This phenomenon is mostly observed from social insects e.g., ants, fireants, bees, or wasps. For instance, *food* is exchanged among adults and larvae in the ants’ trophallaxis process. The ant workers carry baits back to the colony’s nursery. Because adult ants cannot actually digest *solid foods*, the bait is fed to the larvae which digest the material and regurgitate the baits in a *liquid form* back to adult ants. In turn, these ants feed other members of the ant colony. In this manner, ant baits are spread throughout the targeted ant colony. Without trophallaxis the ant bait would not penetrate the *gigantic organism* constituted by the ant colony. The phenomenon is also seen from vertebrate animals e.g., birds or wild dog. For example, bird parents looks for food to store it in their crops when *far away* from the nest. To feed their offspring, they fly back to the nest and *regurgitate* foods to transfer to their young. Trophallaxis is also performed by members of the dog family. In the wild, a hunting dog will regurgitate food *gorged* when far from its lair in order to feed its

puppies. To *trigger* trophallaxis, these puppies *lick* the face of their parents. For domestic dogs, they are tame because of arrested development, and will treat with certain humans, in particular their *owner*, as their "parents". Therefore, a dog may manifest a vestigial feeding instinct when it licks human face.

Besides trophallaxis, *pheromones* [Sumpter et al, 2003],[Payton et al, 2005], act as agents to keep all members within the group. For example, the ant queen produces a special pheromone without which the workers will begin raising a new queen.

In short, "trophallaxis" obtains the meanings of *food reproduction* and *food exchange* while "pheromones" is implicitly recognized as means of communication, *global agents* and *local agents*. In details, 1) ant larvae digesting solid food into liquid form and bee pupa digesting nectar into honey are good examples of the *foods reproduction* phenomenon, 2) bird parents feeding their offspring, hunting dogs regurgitating foods for their puppies, ant larvae returning liquid baits to ants, and ants feeding the others typically manifest the phenomenon of *foods exchange*, 3) ants or bees also lay down their pheromones along their trails as *global agents* to group all colony members together, 4) puppies lick their parents to trigger the trophallaxis of regurgitated foods or nestlings rub their beak to their parents' one as *local agents* for the trophallaxis.

Inspired from the natural phenomena, we have created a system of multiple autonomous mobile robots that is capable of performing energy trophallaxis to sustain robots' life without human intervention. This immediately rises a central question: what are the minimal requirements to achieve energy trophallaxis in multiple mobile robots? Some answers can be found the following section where the meaning of "Randomized Robot Trophallaxis" is clarified.

3.2 The "Randomized Robot Trophallaxis" Concept

The term "autonomous robot" is widely used to define robotic systems to function without human intervention. In fact, people have attempted to build systems, which could operate without human control. However, the term "autonomy" [Ieropoulos et al, 2004] is difficult to assess due to policy of inventors, which are leading to ambiguous meaning in use. In our opinion, a truly autonomous robot is a robot that must obtain two policies: *behavioral autonomy* and *energetic autonomy* in which behavior and energy are closely related. Until now, the term "autonomy" in robotics has mostly been addressed in the sense of "behavioral autonomy" only, not including "energetic autonomy".

In the further perspective, we have paid interest especially to large populations of mobile robots in which each robot is a truly autonomous agent. But, like animal societies, a potential method to achieve entire autonomy is that robots must demonstrate the capabilities of *energy trophallaxis* obtaining two functionalities: the self-refueling energy and the self-sharing energy. However, due to the randomized robot behaviors in large populations, obviously based on assigned tasks, the energy trophallaxis could be *randomized*. That is, the desired robots have to independently perform not only individual behaviors but also cooperative behaviors to achieve energy trophallaxis randomly.

Next we attempt an answer to the question of minimal requirements appearing in the previous section:

Foods reproduction:

Most electronic vehicles are nowadays equipped with rechargeable batteries to power their executions. In particular, for mobile robots, rechargeable batteries seem presently to be the

best solution. Thereby, rechargeable batteries are considered as "foods" and "foods reproduction" is the process of refueling battery stored energy. A few previous systems e.g., Roomba vacuuming² robots, mentioned "foods reproduction" as a docking station where a robot can move back to dock with the station for battery recharging. Unlike the recharging process of Roomba robots, animal trophallaxis includes the exchange of "foods" from one to another other. Inspired from the foods reproduction of animals e.g., *solid foods* digested into *liquid foods*, we create a charging station where hundreds of rechargeable batteries are automatically recharged and available to mobile robots.

Foods exchange:

Like the phenomenon where bird parents feed their offspring, hunting dogs regurgitate foods for their puppies, or ant larvae returns liquid baits to ants, and ants shares baits to the others, "foods exchange" through direct "mouth-to-mouth" contact is the key to achieve *energetic autonomy*. It requires a robot to have a battery exchange mechanism that allows batteries to be exchanged to other robots. Comparing with the method of battery charging, this approach holds the potential for saving much time of electrical energy transfer. However, ants, bees or dogs can exchange/feed its foods to the other if and only if they can find their colony/family members. Similarly, the self-sharing energy process of mobile robots is completely successful if and only if a robot is capable of searching the other and establishing a "mouth-to-mouth" contact with the other. A battery exchange mechanism is purely required to perform the energy trophallaxis through "mouth-to-mouth contacts". Indeed, the former is global agents in a colony while the latter is local agents between two colony members. Features of the agents will be explained in details next sections

Global agents:

Natural stigmergy is a concept to describe a method of *indirect communication* [Payton et al, 2005] in a self-organizing emergent system where its individual parts communicate with one another by *modifying their local environment*. In particular, ants communicate to one another by laying down pheromones along their trails, i.e. where ants go within and around their ant colony is a stigmergic system. However, stigmergy is not restricted to eusocial creatures in growth. For examples, in passive way, birds rely on the earth magnetic field to emigrate in the winter. In active way, a pole-cat marks its own areas by spreading out its feces while another pole-cat enlarges their own area by moving the poops. Inspired from the natural behaviors, we define "global agents" as "agents" that are able to keep communication of all colony members together or to manage their own behaviors in relation with other members in the colony. In our experimental setup, a pre-built grid map on which mobile robots can follow lines is the "classical stigmergy" inspired solution. For the "evolved stigmergy", using external sensors e.g., compass to estimate related orientation among robots, infrared array to detect lines are methods to enable robots being aware of their locations. However, to overcome the limit of "stigmergy", global radio frequency communication may be a good choice to complement *indirect communication*.

Local agents:

Trophallaxis between two colony members is successfully completed if and only if they are able to communicate or activate the trophallactic state in each other simultaneously. For examples, puppies will lick their parents to start the foods regurgitation when they are hungry. Thereby, licking or rubbing are local agents between two individuals engaged in trophallaxis. Similar to the dialogue of animals, a line of sight infrared local communication

² See www.irobot.com

complemented by contact detection systems within each robot is typically required for trophallaxis process to be successful.

In particular, we have developed a new prototype of robots, named CISSbot capable of performing energy trophallaxis in three forms: robots with mother-ship, robots with robots, and robots with their child. In other words, the robots are capable of carrying out not only energetic autonomy but also behavioural autonomy. The realization of the robots is on the one hand expected to redefine the definition of "autonomy" in robotics. On the other hand, the unique design can suggest a new method to generate truly autonomous robots in large populations.

3.1 Simulation of Randomized Robot Trophallaxis

In this section we address simulated results of energy trophallaxis in terms of self-refuelling energy and self-sharing energy. Like animal life, we assume that a group of mobile robots share a nest, that is, a charging station where they can come back to refuel energy. A simulation setup can be seen in figure 5. The simulation state is shown in four windows (from left to right): Motion, Energy Distribution, States of Energy, and Tasks.

We firstly establish an energy model for single robots. Obviously, battery measure is the best way to estimate the remaining energy of a robot at an instant. However, because the energy consumption model is not uncertain to every robot due to its own mechanism, control, assigned tasks, etc., it is hard to model battery measure for a robot. Therefore, we temporally choose Peukert's discharging function $C = I^{k_t}$ where k is supported by the battery manufacturer since the function is close to the linear equation of experimental power consumption of a mobile robot

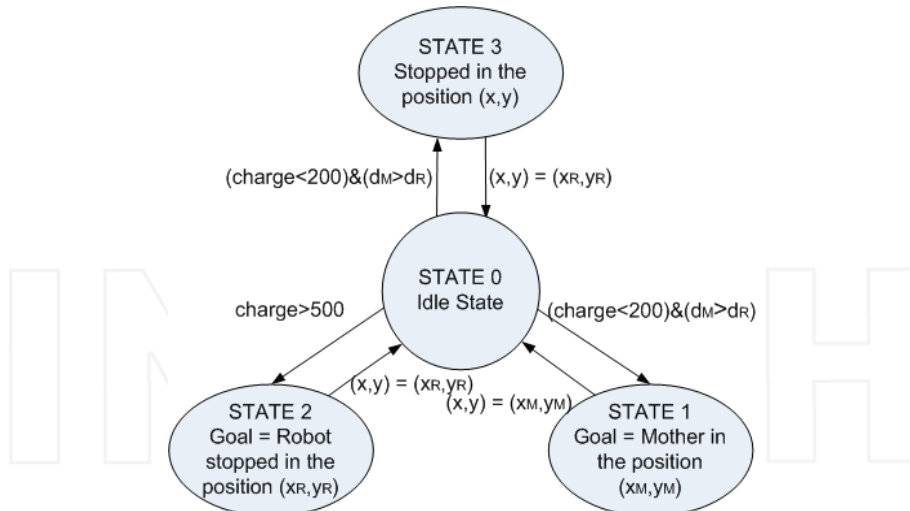


Figure 5. Model of single robot

Basically a robot is initialized with 800 energy units (**eu**) corresponding to the 8 battery holder of every robot. The robot consumes a specific amount of energy, using Peukert's equation, for each step. We propose 4 energy states of robot corresponding to behaviours and energy states:

- State 1 is an interaction between a robot and the mother charging station in the organization. A robot has to go to the mother charging station to refill energy if its energy is less than 200 **eu**, and by default, it has a higher priority to go to the mother charging station.
- State 2 is an interaction between two robots on demand in a organization. A robot is able to exchange 100 **eu** with another robot demand if its energy amount is more than 500 **eu**.
- State 3 is also an interaction between two robots in organization and their interaction with the environment (for example, due to an assigned task), but it is different from the State 2. A robotic agent will stop to wait for another robot coming to share 100 **eu** if its energy is less than 100 **eu** and it is impossible to go to the mother charging station due to its estimation of the relative distance and remaining energy.
- State 0 is an interaction between a robot and its environment (for example, obstacle avoidance among robots, and between robots and lateral walls). A robotic agent is autonomously free to explore in order to consume energy.

To approach a solution for battery exchange quickly, we suppose a coordination algorithm for the multi-robot system based on two phases: path planning and battery exchange. The algorithm is proposed to emphasize the interaction of agents irrespective of their surrounding environment which should be taken into account in practice.

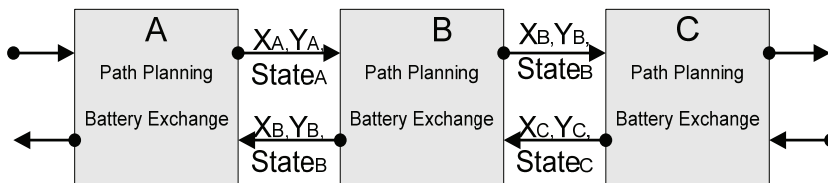


Figure 6. Model of multi-robot system coordination

Briefly, each robot has its own battery exchange supervisor. The supervisor collects input data from the robots, e.g., the current coordinate (X,Y) and the current energy state STATE; deals with this updated data; and issues output commands, e.g., NEXT STATE of energy, goal coordinate (Xgoal, Ygoal). A more detailed algorithm of the battery exchange executes infinite loops of comparisons of energy states and current positions among the robots as well as the robot with the mother, in order to give commands about what the robot should do next (the goal of the robot). Meanwhile, the path planner guides the robot to reach the directed goal and update the next position, which is used as feedback for the battery exchange algorithm to compute the next states (fig.6) Detailed information of the simulation setup can be found in [Ngo et al, 2007].

Firstly, inspired from the instinct of self-preservation in ant colonies where worker ants return to the nest to eat a liquid foods produced by the larvae, a simulation of self-refuelling energy is performed to demonstrate the capability of self-refuelling energy. Secondly, like feeding of bird or dog parents to their offspring, we establish a simulation to demonstrate the capability of self-sharing energy among robots. Thirdly, we examine a combination of self-refueling energy and self-sharing energy to point out an efficient solution for energetic

autonomy in mobile robots. Finally, we discuss problems related to meaning of “randomization” in terms of initializations, motion, and energy distribution.

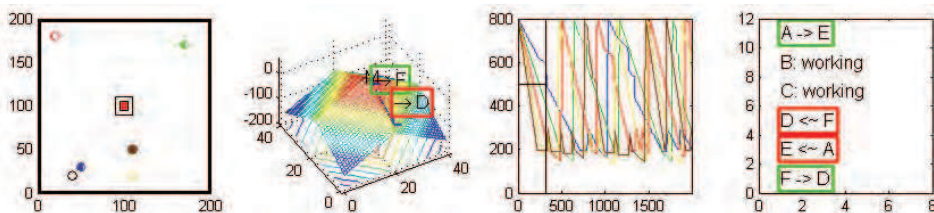


Figure 7. Simulation screen: Motion (over left), Potential of Energy (left), States of Energy (right), Tasks (over right)

Firstly, inspired from the instinct of self-preservation in ant colonies where worker ants return to the nest to eat a liquid foods produced by the larvae, a simulation of self-refuelling energy is performed to demonstrate the capability of self-refuelling energy. Secondly, like feeding of bird or dog parents to their offspring, we establish a simulation to demonstrate the capability of self-sharing energy among robots. Thirdly, we examine a combination of self-refueling energy and self-sharing energy to point out an efficient solution for energetic autonomy in mobile robots. Finally, we discuss problems related to meaning of “randomization” in terms of initializations, motion, and energy distribution.

3.3.1 Self-refueling Energy Based on “Food Reproductions”

A simulation of 2000 running steps is set up to examine how many time robots need return to the charging station to refuel their energy. To model energy consumption we assigned different energy cost functions for every robot as the Peukert’s equation. Virtual pheromones based on Euclidean distance are used to guide robots to the charging station placed at the center of scenario. Every robot is continuously managing its resources by estimating remaining energy, but not estimating the distance from its current position to the charging station.

Initially, robots are equipped with fully charged batteries and randomly deployed in the scenario. The robots are freely moving around to spend energy based on energy cost functions and returning to the charging station when energy is low. Table 1 shows the record of number of energy refuelling events in 2000 steps, which can correspondingly calculate the total energy consumption of each robot with respect to energy state. Truly, the result corresponds to the energy cost functions (workloads) assigned to individual robots, which are increased from A to E. In the scenario of 200x200 unit (shown in figure 7 over left), a robot equipped with 800 **eu** maximum has possibility to come back because it is in the energy potential itself. However, some robots die when the scenario is enlarged. The death sometimes happens once robots far way from charging station do not have sufficient energy to return to the charging station. Death rate reduction of robots when their energy is expired while working far way from the charging station was partly discussed in the modelling and will be clarified further next section.

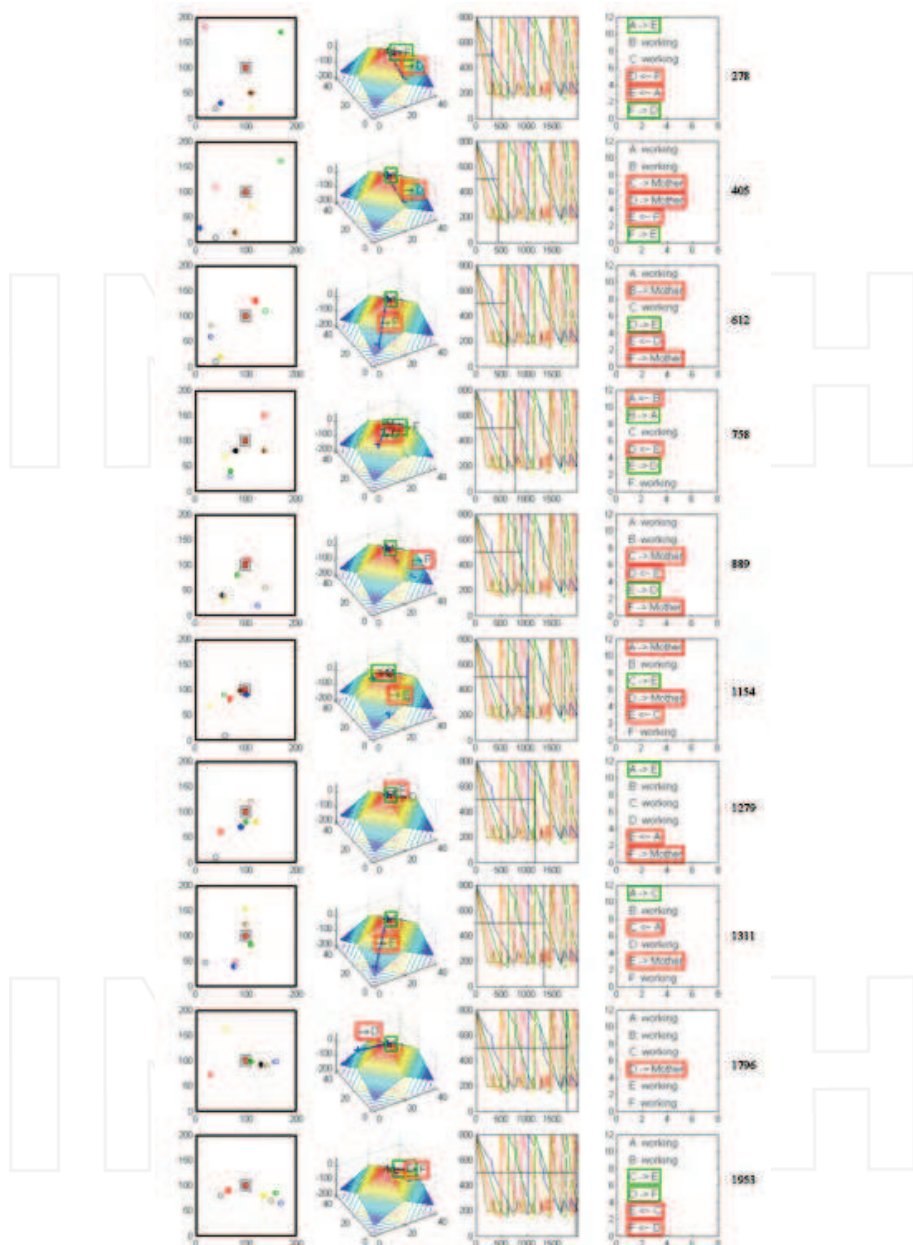


Figure 8. Snapshots of simulation on time scale

	A	B	C	D	E
Back to CS	3	5	5	6	7

Table 1. Simulated result of 5 robots in 2000 steps: Self-refueling Energy

	A	B	C	D	E
Survival time	5.4	4.2	1.1	3.4	5.4
Sharing Battery	0	0	1	0	0
Receiving Battery	0	0	0	0	1

Table 2. Simulated result of 5 robots in 2000 steps: Self-sharing Energy

	A	B	C	D	E	F
Back to CS	2	3	4	5	6	8
Sharing	1	3	0	1	0	2
Receiving	0	0	2	1	2	2

Table 3. Experiment of 6 robots in 2000 steps: Combination

	A	B	C	D	E	F
Back to CS	3	4	5	7	10	13
Sharing	2	1	2	3	3	3
Receiving	1	1	3	3	2	4

Table 4. Experiment of 6 robots in 4000 steps: Combination

3.3.2 Food Exchange: Self-refueling Energy & Self-sharing Energy

Observed from the experiments of self-refueling energy described in the last section insufficient energy to return to the charging station causes robots to die. This enables robots to limit their activity domain since the further the robot is away from the charging station the harder the robot is able to survive. On the other hand, if every robot must go back to the charging station when energy is exhausted, they spend too much time and energy by travelling back. Moreover, density of traffic is accordingly increased causing traffic jam on the road as well as at the charging station, leading to prevention of energy refuelling.

To compensate drawbacks of self-refuelling energy, a solution of self-sharing energy is proposed. The solution enables each robot to become a mobile charging station to rescue other robots through battery exchange.

To test capability of self-sharing energy, we apply the policy of self-sharing energy only to 5 robots with different energy cost functions and deploy them randomly in the scenario without a charging station. From simulation result, we have had a statistic number of energy exchange and survival time as shown in table 5. It is observed that energy cost function of robot C is less than the one of robot A or robot B, but robot C dies earlier than robot A or robot B since it has shared energy with robot E. Thanks to energy aid of C, E survives longer than the other while its energy cost function is the most heavy. Although robot E is energetically rescued to prolong the life, no robot survives after an interval since external power resource is not provided. The example illustrates that the capability of self-sharing energy is aware as a short-term energy while the capability of self-refueling energy is understood as a long-term energy.

A combination of short-term and long-term energy solution enables robots to prolong their life, save energy and time of traveling back to charging station, avoid traffic on the road and

collision at the charging station. An example of 6 robots with both capabilities is examined to evaluate survivability of mobile robots.

For the first trial, we executed the simulation in 2000 steps illustrated in figure 8. Astonishingly, there is no dead robot in 2000 steps. In fact, robots all use short-term and long-term energy to support or refuel energy cooperatively. A statistical table of simulated results can be seen in table 3. Given example of robot D, at instant 278, D is shared energy by F, and then D has enough energy to go back the charging station to refuel energy at instant 405. It is surprising that D turns into a mobile charging station at instant 612 when it is going to share energy to E. But, after energy of E is refreshed at the charging station, E is going to share energy to D again at instant 758 and 889. Likewise, D still survives at step 1796 and will go back to the charging station. About 200 steps latter, D with full energy capacity is going to rescue E and so on.

Similarly, the simulation was executed 4000 steps again. Simulated results in table 4 demonstrate that the combination of self-sharing energy and self-refueling energy is a novel promising solution for groups of mobile robots towards energy autonomy.

4. Hardware Design for Energy Trophallactic Robot

4.1 An Introduction

The term "autonomous robot" is nowadays widely used to define robotic systems which function without human intervention. In fact, people have attempted to build systems which could operate without human control. However, the term "autonomy" is rather hard to assess due to the policies of inventors, which are leading to ambiguous meanings. In our opinion, a fully autonomous robot is a robot that must poses two qualities: *behavioral autonomy* and *energetic autonomy*. Behavioral autonomy can be defined as the ability to determine and execute actions which could be affected by the obtainment of energy. Energetic autonomy can be seen as the ability to maintain its energy to prolong its lifetime. However this behavior can be used to yield energy in the case of an energy self-rechargeable robot. To date, the term "autonomy" in robotics has mostly been used in the sense of "behavioral autonomy" only, not including "energetic autonomy". The example given is an intelligent battery-operated robot that can carry out a task without human intervention. e.g., iRobot Roomba vacuuming robot³. However, when working on an assigned task, the energy of the robots must previously be estimated to complete the task over some predefined period. In this period, the behavior of the robot may be considered as an autonomous operation. Otherwise, without human assistance to complete a job, the robot must autonomously return to a charging station, if possible, to refuel when the battery becomes low. In short, the behavior of the robot is always under the constraint of energy.

In the longer perspective, we are interested in large populations of mobile robots in which a robot is a truly autonomous agent. However, to achieve full autonomy, the robot must demonstrate the ability of energy trophallaxis obtained from two functionalities: self-recharging energy and self-distributing energy, accompanying the ability of behavioral autonomy. Conversely, energy trophallaxis powers essential elements of the behavior, including sensing, motion, and computation in order to maintain the robots' action.

In particular, we have developed new robots, named CISSbot, that can perform not only energetic autonomy, but also behavioral autonomy, concurrently. The realization of the

³ See www.irobot.com

robot is on the one hand to redefine the definition of “autonomy” in robotics, and on the other hand, the unique design can suggest a new method to create truly autonomous robots in large populations.

4.2 Related Work

In the section, parts of related work of behavioral autonomy and energetic autonomy will be addressed. On the one hand, the overview is to emphasize the importance of energy trophallaxis in large robot populations since there does not yet exist a truly autonomous robotic system. On the other hand, we will explain the technical details that we have taken into consideration to design our robots. From this viewpoint, we have chosen some types of robots as examples since their designs bear the closest similarity to our design specification. For behavioral autonomy, it is easy to search for a list in terms of self-reconfigurable robots and behaviorally autonomous robots. The former is defined as a machine built from several identical modules, and by reforming their module connections to change the shape and functionality of the entire machines or organism. The M-TRAN [Murata et al, 2000],[Yoshida et al, 2001] and ATRON [Lund et al, 2005][Ostergaard et al, 2004] reconfigurable robots are typical representatives of the class. The M-TRAN uses magnets to attach surfaces of modules together and Shape Memory Alloys (SMAs) to detach those connections. The ATRON sets up a point-to-point physical connection by using the hooks of the active connector to grab into the passive connector. M-TRAN modules are battery-powered units but they are not able to share or self-recharge energy automatically, while the ATRON modules are also battery-powered units that are able to share energy by inter-connections. However, M-TRAN and ATRON both still meet the limit of energetic autonomy, and thus they are only self-reconfigurable in morphology, but not self-rechargeable. The second requirement of behaviorally autonomous robots is an autonomous robotic system operating autonomously without human intervention in behavior. Although this exists in many single robots, and in cooperative or coordinating robots in a wide range of applications for underwater, ground, or aerial environments, we have chosen Swarm-bots [Groß et al, 2006][Mondada et al, 2005] as a good example since the robotic system covers numerous features similar to, or more advanced than, the other systems. Swarm-bots (s-bots) is a European project to create self-assembling and self-organizing robots inspired by from social insects or other animal societies. Unlike M-TRAN or ATRON, s-bot is a completely independent mobile robot, that is, s-bot is able to move without the need to inter-connect with other s-bots. For capabilities of self-assembling and self-organizing, s-bots are equipped with a flexible gripper that is capable of grasping another s-bot to lift it when it needs to pass over large holes or pass through narrow passages in complex environments. They also have two short rigid grippers to provide easy connectivity to the other robots. In combination with two kinds of gripper, several types of sensors are used to play very different roles in swarm-robot configurations, e.g., infrared proximity sensors, infrared ground proximity sensors, color sensors, inclinometer sensors, humidity and temperature sensors, etc. In fact, Swarm-bots are a type of battery-powered robot. Unfortunately, the swarm-bot has no capability for sharing energy among robots, or refueling its energy by exchanging batteries with a charging station, eventually they would be able to perform such capabilities thanks to very high processing power, excellent sensing capability, and smart grippers. In short M-TRAN, ATRON, and Swarm-bots are not yet truly autonomous robots.

However, features of physical connections, neighbour communications, and processing power are very useful examples when designing the CISSbots.

For energetic autonomy, there exist only a few robots that are able to act as energy rechargeable robots or self-power robots. A very good example of the first class is the vacuum cleaning robot of which Roomba and CleanMate are two typical representatives. Typically, the robots move around freely to clean carpets and automatically return to the docking station to recharge the battery when it is low. Although the robots have partly solved the problem of self-recharging energy, they still lack the capability of quickly recharging by exchanging batteries instead of waiting at the charger for a long time. Also, the robots can only work alone without capability of sharing energy among moving robots as our CISSbots do, so they can not act in large populations. A well-known robot of the second class is a series of ecological robots named EcoBot. These robots are referred to as a class of energetically autonomous robots that are self-sustainable by collecting their energy from waste in the environment. EcoBot-I [Ieropoulos et al, 2004] was developed to utilize sugar as the fuel by onboard Microbial Fuel Cells (MFC), while EcoBot-II [Ieropoulos et al, 2005] was created to consume dead flies, rotten fruit, and crustacean shells. The application domain of EcoBot is places which are very hard to access by humans, e.g., under water or in a poisoned area. In fact, the EcoBot series has partly overcome the problem of self-powering, but they can only work in a waste environment where biomass is available. Moreover, like the vacuum clearing robots, the EcoBot usually acts alone, so it can not be able to benefit from colony activities.

4.3 The CISSBOT Design Idea

As a part of our research into sociable robots, we are currently developing a prototype of a truly autonomous robot, called CISSbot (shown in figure 9). The CISSbot is a differential two wheeled robot with a special mechanism of battery exchange. The architecture of the CISSbot is divided into two main parts: the lower layer and the upper layer. The lower layer is the behavioral control to perform the behavioral autonomy while the upper layer supports battery exchange to refuel the robot's energy or to share energy with the others.

Like mobile robots working in 2D, the lower layer of the CISSbot also has a full specification of sensors, actuators and a central processor to control the robot's behavior automatically. However, because of our target to demonstrate energy distribution in large populations, we simplified the experimental scenario to a grid map. Thereby, the behavioral control enables the CISSbots to move freely on the grid map, meeting each other at a point, or moving back to a charging station.

However, unlike mobile robots seen previously, we have been developing a battery exchange mechanism for the CISSbot to load and unload batteries. The mechanism is designed in an H-shaped set of battery holding boxes that include the electrical contacts and the battery pushing systems at both sides. However, in order to make a decision about the battery exchange, the electronics of energy management have to be taken into consideration. More details are described in the next sections.

This design is a compromise between several mechanical, electronic and control considerations. To cause a robot to exchange batteries with the charging station, or to distribute batteries to other robots, the behavioral control and the battery exchange mechanism must collaborate in a synchronized mode.

In order to realize energy trophallactic robots in large populations, we require a robot to:

- sense the current state of its energy;
- give a decision about energy replenishment;
- search and talk with other robots;
- have neighbor to neighbor communication;
- be able to contact or bump the charging station or other robots precisely;
- have a mechanism to exchange the battery successfully.

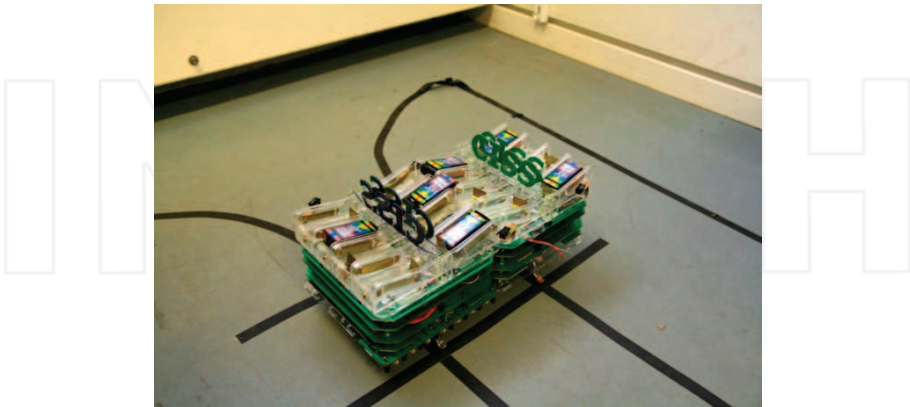


Figure 9. Two robots in a battery exchange process

4.4 Hardware Realization

The goal in designing the CISSbot is an experimental platform of an energy trophallactic robot, so we decided to develop the robot in layers and modularity. That is, the system and its functionality can be extended by just adding new layers onto the base layer, or plugging new modules onto the other electronic boards. The rest of the section will realize several aspects of the mechanical design in multilayer architecture, modular functions of electronics, and how to assemble parts into a compact platform.

4.4.1 Mechanical Design

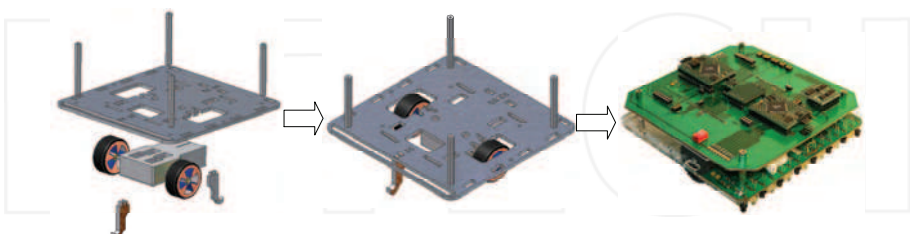


Figure 10. Mechanics of the behavioral control layer: CAD disassembled (left), CAD assembled (middle), completed mechatronics (right)

Mechanics of Behavioural Control

Towards an easy process of battery exchange, the CISSbot is physically formed in a 15 x 15cm square shape. Like most mobile robots, the chassis of the CISSbot is a base to hold the motion mechanism and electronic system to control the robot. The movement of the CISSbot

is driven by a differential two wheeled system and two castors to keep the robot balanced. Initially, we selected the gear-box of two DC motors from Tamiya toys, but the test showed that the gear-box can not be used since its power consumption is over 800 mA, while we are using 250 mA batteries to power the robot. Therefore, we have modified servomotors into continuous servo motors at a gear rate of 218:1 to drive the two wheels because such motors allow the CISSbot to move quickly in a narrow space, to turn slowly around its central point, and to approach easily to a target at a stable current of 100 mA approximately.

The mainboard to control the CISSbot's behavior is put on the top of the base. At two sides of the base chassis, an odometer of the two wheel encoders is mounted to observe the movement of the wheels. The base is made as compact and robust as possible, with the main emphasis on the low-cost production.

Mechanics of Battery Exchange

The mechanism of battery exchange is a complicated architecture. To protect against short-circuits, flexible plastic is the material chosen to compose the architecture. In particular, the skeleton of the battery exchange mechanism is assembled from several flexible plastic parts to form 8 battery boxes on the base. At the two sides of each box, there are two brass plates to physically conduct electricity from the batteries to the entire system. To hold a battery in the battery box, as well as to protect against mechanical shocks when the robot is moving, a plastic pad is tilted 12.5 deg over the central base (see figure 11). Each battery box involves a linear motion mechanism fixed at the two ends of the box in order to allow the mechanism to push the battery in the slide-way. As expected, initially, it was very hard to find a compact linear motor mechanism since there is no geared micro motor available. Fortunately, we found a geared micromotor, rate 25:1 with excellent specification from www.solarbotics.com. After being technically modified, the microlinear mechanism was made manually to ensure that it is powerful enough to force the battery out.

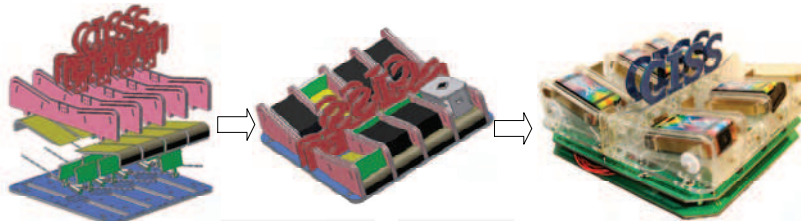


Figure 11. Mechanics of the battery exchange layer: CAD disassembled (left), CAD assembled (middle), completed mechatronics (right)

Under the base of the battery exchange, the entire battery management, control of 8 battery boxes and local communication for the battery exchange process is physically hung (see figure 10, right). In the future, we will redesign the battery layer to hold a laser-sensing system on the top for the robot's further sensing capability.

4.4.2 Modular Electronics

Power Management

The goal of the CISSbot is to lead to a new methodology for a truly autonomous robot, so power management is the key to our considerations. The main requirements of the power management system are to continuously sense the current state of the batteries carried by

the robots, protect against occurrence of the short-circuits, regulate the power of the source of usable energy for the robot's actions, and select the number of batteries in use.

As shown in figure 12, because the batteries used are of rectangular parallelepiped form with two brass connectors modified at each side, the battery exchange process could randomly lead to the wrong sign connection when the battery is shifted another robot or from the charging station. To solve this problem, we added a two way rectifier to ensure the right polarity, no matter how the connector side of the battery is electrically conducted on the electronics board of the power management system.

In moving towards a smart energy management software program for the CISSbot, the input data of the current state of the battery is very important, and inquiries about the updating speed, the current and the reliability of the measured data are strongly emphasized. However, depending on the chemical characteristics of the rechargeable batteries, e.g., Li-Po, Li-Ion, Ni-CD, Ni-MH, etc., their capacity is changed differentially, and thus their discharging functions are not identical. This makes battery monitoring more difficult and less precise if only the voltage of the battery is measured, which is what many battery monitors have done previously. Moreover, load of the system powered by the battery probably affects the measurements, and the limit of the deliverable current. The question is, how to monitor the current state of different types of the battery precisely in real-time. To improve the accuracy of energy management, the methodology of monitoring both the current and the voltage of the battery has been selected. Fortunately, our method has also been the considered by Maxim electronics offering a commercially available smart battery monitor chip. We needed to connect only one wire of the chip to our processor in order to evenly monitor the elements: voltage, current, and temperature.

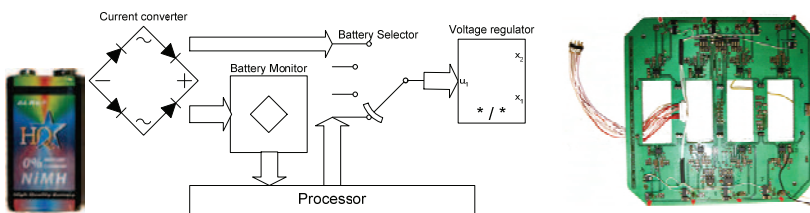


Figure 12. Power management: Block diagram (left), completed PCB (right)

The voltage regulator of the power source is also very significant for the modular electronics of the CISSbot since there are many different modules powered by a single source. Because the CISSbot's electronic modules are operating in a large voltage range from 3.0 V to 9.0 V, a series of voltage regulators has been implemented. Unusually, we had to specially select two high-current regulators for the two drive motors of the wheels owing to the heavy load.

To make the power management more flexible and powerful, an electronic circuit of battery selection controlled by the processor was added on. The selector allows the power management system to decide the number of batteries in use with respect to the power consumption of the CISSbot in an execution mode, as well as the current state of the batteries on the energy base. For example, in free motion mode, the CISSbot needs to be powered by two fully charged batteries, but there are currently only five partly used batteries, which might be exchanged by the other robots on the base so that four of those are

fully activated at once. This helps the CISSbot to use the remaining energy from all batteries used.

The elements of power management described above is entirely mounted on a single printed circuit board (PCB) that is held under the mechanics of the battery exchange layer (see figure 12)

Processing Power

Since the CISSbot architecture is structured on two layers, the behavioural control layer and the battery exchange layer, we decided that each layer should be powered by a processing unit instead of having a central unit for the entire system. This division aims to increase computational power in each unit, as well as to reduce unnecessary signals passing through two processing units. If the processing power was put in a single unit, several electrical signals would have to be processed, filtered, and transferred to related devices simultaneously, leading to overloading of the processing unit. In addition, information propagated between two processing units must be preprocessed and filtered to avoid a traffic-jam on the common bus, leading to transmission delay.

As illustrated in figure 13, the behavioural control layer is controlled by an ATMega128 microcontroller, named the main processor, and the battery exchange layer is driven by an identical micro-controller, named the secondary processor. ATMega128 from Atmel is a 8-bit micro-controller with 128 Kb flash memory, 4 Kb RAM and 4Kb EEPROM. The microcontroller is set up to run at 14.7456 MHz.

The main processor is on the one hand responsible for several sensing devices to control the CISSbot's behaviour: an infrared array (line-following sensing), a compass (orientation sensing), an odometer with two wheels (distance estimation), and wireless communication (global signal propagation). On the other hand, the processing unit also drives the two differential motors of the motion mechanism.

The secondary processor is mainly responsible for monitoring the state of the batteries. In addition, the local infrared communication (neighbour communication) of the battery exchange process and the control of the microlinear motors to push the batteries are also managed by this processor. Assisted by the main processor to control the CISSbot's behaviour, proximity based on the same local infrared sensors can be detected by the secondary processor in order to build a local map. In association, the two processors are able to intercommunicate on a TWI interface based on I²C protocol.

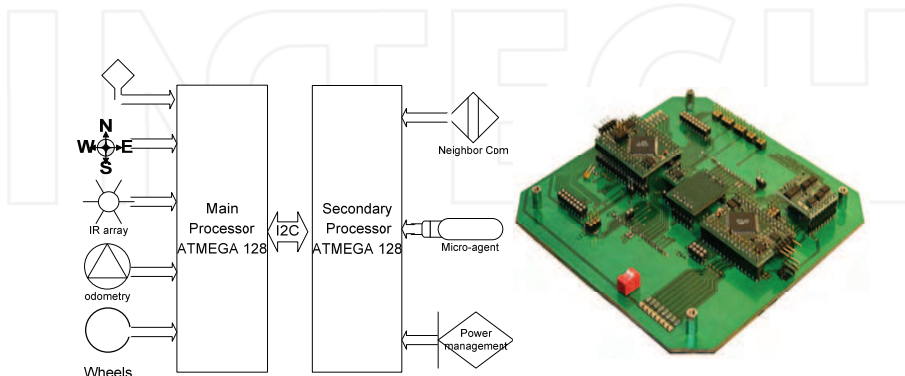


Figure 13. Processing power: block diagram (left), completed board (right)

Sensor

Line following sensor:

As the CISSbot is an experimental platform of a truly autonomous robot, we set up a grid map scenario of white crossing lines on a black carpet. To approach quickly to the goal of battery exchange, a highly accurate infrared array has been made to control the motion mechanism of the CISSbot adaptively. However, unlike most of the infrared arrays available on the market, we applied high computational power using the Lagrange interpolating polynomial in order to find the distance measured from a white line to the central point of the robots precisely. The measured values are converted to numerical values by the on-board ADC port of the microcontroller. The infrared array is also able to calculate the varying distance from the center to 10^{-2} mm accuracy. The numerical value of the varying distance is used to apply the proportional – integral – differential (PID) controller for CISSbot motion.

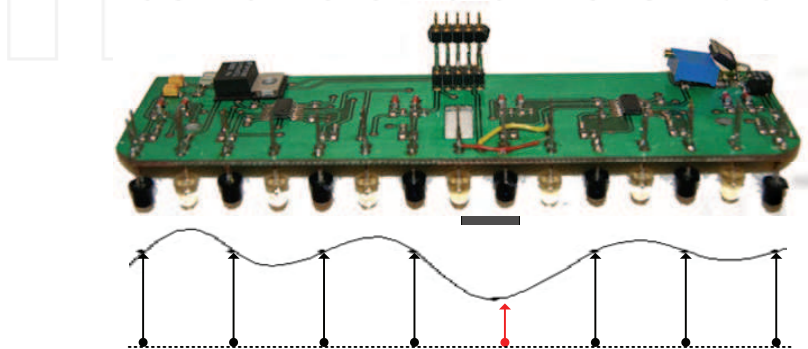


Figure 14.. Top. Line following infrared array. Bottom: Correlative Lagrange interpolating polynomial

Orientation sensor:

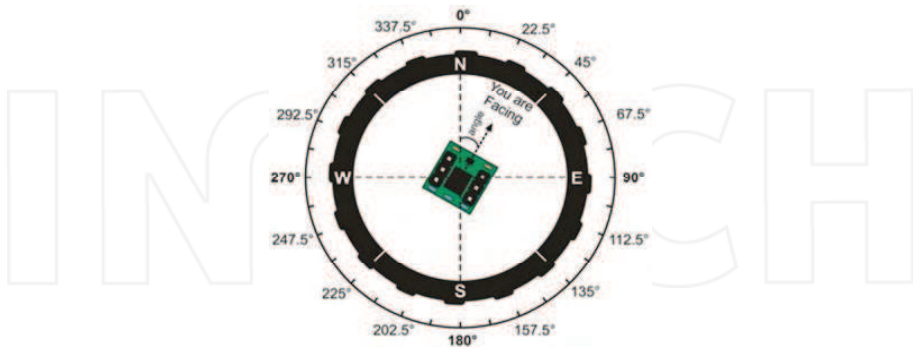


Figure 15. Digital compass

In addition to sensing information, a CISSbot is equipped with a digital compass: a dual axis magnetic field sensor built round the Hitachi HM55B IC. The external device is used to determine the orientation of the robot upon the Earth's magnetic field with sensitivity up to

microtesla. This information is essential to calculate the related orientation among the moving robots in order to compensate for the inadequacy of their orientational sensory information. In particular, it is very useful for the battery exchange process when two robots are in preparing to exchange batteries. Although we are currently using the compass to sense bidirectional axes only, it will be more useful in the future, with high sensitivity, to guide robots approaching each other when we remove the grid map.

Odometer sensor:

For further sensing, a CISSbot is also set up with a couple of incremental encoders for both wheels. By using Hamashuta (very short-range infrared), the encoder will increasingly accumulate the travelling distance by observing a barcode, which is fixed on the wheels, when the wheels are rotating (see figure 16). In the current design, the sensor is able to sense 2 mm along the distance of the robot's movement. The distance information captured by the width of on-off pulses by the microcontroller is used to guide one robot to approach another one for battery exchange very precisely, or to estimate energy consumption, and to propose a schedule for energy management.

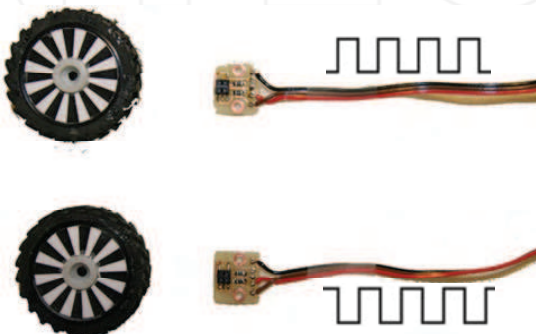


Figure 16. Odometer: barcode (left), short-range infrared sensors (right)

Proximity distance sensor:

To perceive the surrounding environment, distance sensors are indispensable. However, in a large population of homogeneous mobile robots where interference with signals always happens, long-range sensors are not absolutely appropriate, and primitive short-range sensors are better. Further, the signal interference is reduced if a high-speed sensor is chosen. Based on the required specifications, infrared is the best choice in this case. At the each side of the CISSbot, four pairs of proximity infrared sensors are disposed as illustrated in figure 17. The current design allows sensing up to 16 cm in front and on both two sides of the CISSbot approximately. The purpose of this sensing is to report if the robot meets obstacles, or recognizes other robots.

Neighbourhood Communication

In order to have a successful battery exchange process, every robot must be able to communicate with its neighbouring robot. To obtain this communication, each side of the CISSbot has four sets of infrared diodes and phototransistors, corresponding to the location of the four battery boxes on the sensor board. A diode for transmitting messages and a phototransistor for receiving data are placed according to the center of each battery box. With the infrared couple placed in this pattern a robot can communicate with a neighbouring robot if they are closely approaching side by side. Based on the number of

infrared couples in communication, the two robots negotiate to decide in which battery box of the sharing robot the battery is handed on, and which battery box receives such a battery on the receiving robot.

For the possibility of high-speed communication, we initially designed the communication with four infrared couples transmitting data from one robot at the same time, and then the other robot should be able to receive four independent signals at any given time. These couples all were directly connected to the processor in order to be driven by four identical set of UART software. Unfortunately, the test showed that the speed for a single channel would be always less than 735 bps. Thus, one robot must take a longer time to negotiate with another one in order to complete the battery exchange process. However, the need for high-speed neighbour communication to avoid traffic-jams in large populations is highly urgent, so $(\sum_{i=1}^n + 1)^4$ times 730bps is not a promising result. We changed our minds, and used the built-in UART of the processor in combination with a multiplexer. In fact, the four pairs of infrared sensors were multiplexed by an analog multiplexer, shown in figure 17. Although use of the multiplexer for neighbour communication could limit the number of communications to a neighbour at the same time, it increases the transmission bandwidth to 9.6 kbps. As a result, neighbour communication is raised to 2.4 kbps approximately.

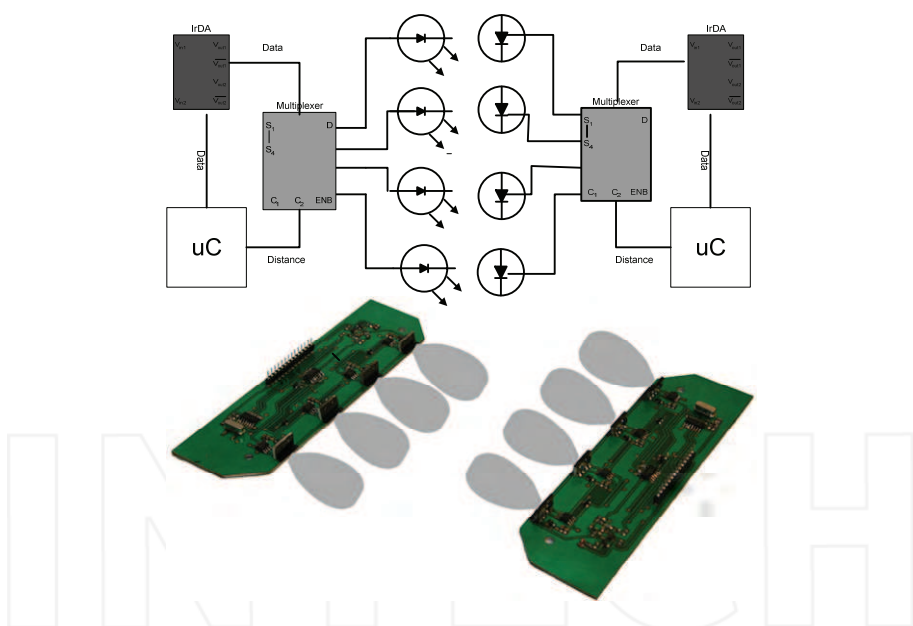


Figure 17. Neighbor Communication: block diagram (Top), completed boards (Bottom)

To ensure reliable propagation of data between two neighbors, an IrDA physical layer is placed between the UART and the infrared sensors for encoding and error checking. The data received from the standard UART is encoded, and output as electrical pulses to an

⁴n is the number of neighbor communication units in communication, maximum 4. 1 plus is to send a command of starting the battery exchange process.

infrared diode transmitter. If infrared phototransistor receivers also capture data which are output as electrical pulses, the physical layer demodulates these electrical pulses and transmits to the UART of the processor. Because the modulation and demodulation method is performed according to IrDA standard specifications, it allows a user to interact with the CISSbot using a portable device, e.g., a cellular phone, a laptop, or any other device with an IrDA interface.

Global Communication

As described above, neighbor communication can assist a robot to communicate with other robots at very short range only. Nevertheless, the CISSbot is a energy trophallactic robot in large populations, and thus global communication at long range is certainly required to search for and talk with other robots. In this request, wireless communication is the best choice for low-cost, wide range, and ultra-low power consumption. Initially, we selected CC1000 from Chipcon for our robots. However, a highly complicated circuit board is needed for this device, and its frequency is not in the EU licensed range. Hence, we have finally chosen CYWUSB6935 from Cypress for the global communication. The wireless chip is easily integrated into the processor, with few extra components. This utilizes the worldwide unlicensed 2.4 GHz ISM frequency band and uses a robust Direct Sequence Spread Spectrum (DSSS) transfer method with a data rate of 62.5 kbps and a 50 m range. The low standby power consumption of $<1\mu\text{A}$ is ideally suited for battery-powered robots. Fortunately, the wireless board is available from the Chip45⁵ company.

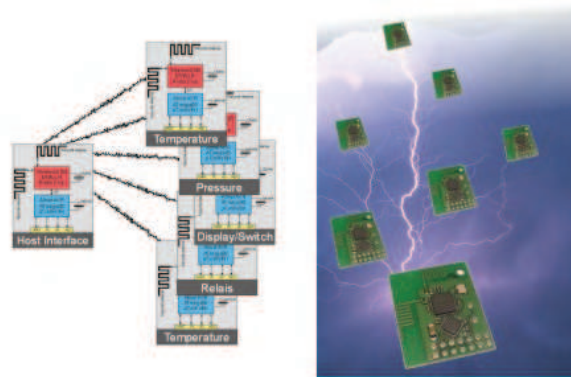


Figure 18. Global communication: (N:1) Wireless Network

To ensure reliability in bidirectional communication between one CISSbot and another, a set-up of wireless multipoint-to-point (N:1) networks was implemented. This protocol aims beyond the classical solution of point-to-point (1:1) wireless communication. Error-detection, correction, and automatic channel selection are additionally programmed into the processor. The propagation protocol guarantees that a robot will receive necessary information on the battery state, and commands about the communal jobs from other robots, as well as broadcast its own information to the others.

Driver of Behavioural Control

⁵ The boards are bought from chip45.com. (N:1) protocol was initially a firmware of the website. However, this protocol is mostly modified in order to apply for our robots.

Basically, two DC motors of the motion mechanism are driven by Pulse Width Modulation (PWM) signal sent from the main processor. As the most popular control algorithm used to control a mobile robot is a PID controller, we also apply this method to the CISSbot with an external feedback of the varying distance of the infrared array and odometer information from the wheel. The power electronics used to control two wheeled motors are a dual H-bridge driven by a micro-controller. This allows the CISSbot's motion mechanism to be controlled by the UART of the main processor.

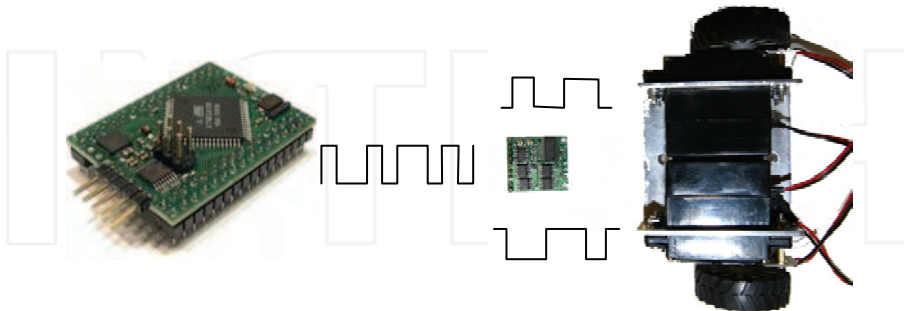


Figure 19. Driver of two wheeled motors

However, the CISSbot executes a lot of action modes, e.g., free mode, collision detection mode, job mode, battery exchange mode, and so forth, and a basic PID controller might not respond well to these differential behaviors. To adapt the control to each mode, the controller must be upgraded to an adaptive PID whose setpoint and gains are adaptively changed according to each mode. For example, the gain might be large in the free motion mode to allow the robot to run quickly, but it should be minimal value in the battery exchange mode to make the process successfully.

Driver of the Battery Exchange

The battery exchange mechanism is a set of eight linear DC micro-motors systems, manually constructed in a combination of linear micro-motors and screw thread rods. This allows the rotating force of the DC micromotor to transform the pushing force of the screw thread rods in order that a battery is physically pushed from one robot's battery box to the other if the two robots are completely aligned side by side. However, it is too wasteful to use eight H-bridges to drive eight motors, instead of multiplexing them in order that they can be controlled by a single H-bridge motor controller. The solution confronted the barrier of the capability of a multiplexer to deliver a high current to the DC micromotors. Referring to the specifications of the micromotor (3 V, 128 mA), no fully suitable multiplexer is available on the market. Therefore, to overcome the problem of high current conductivity, we used a digital multiplexer to switch the mode of the micro-motor. However, the current to control the micromotors goes through high power FET transistors under control of the H-bridge. Because we used a single H-bridge, a UART and 3 address lines of the secondary processor are needed to drive the pushing mechanism of the eight battery boxes. In fact, a battery exchange process takes 5.7 s to perform, and it consumes 0.7 joule to deliver a force of 80 N approximately, when the micromotor is powered by 3.3 V at a current of 120 mA.

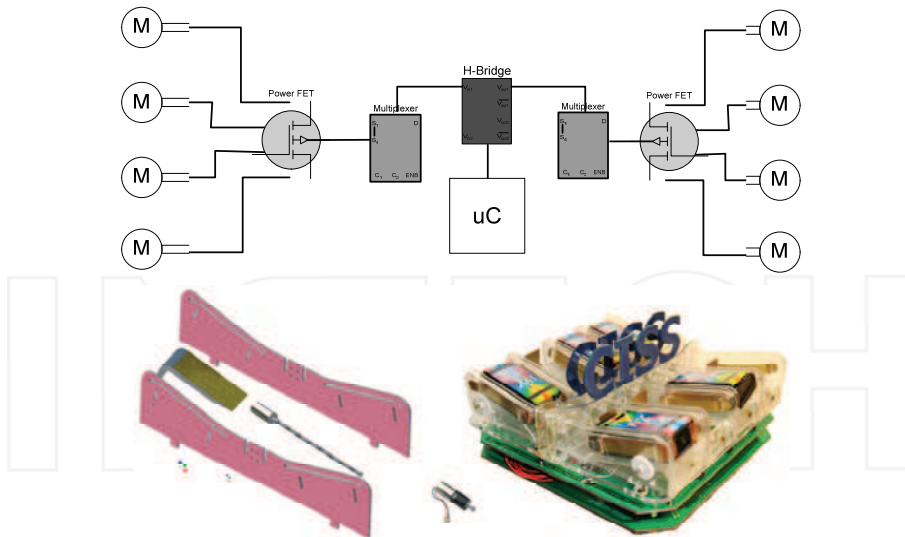


Figure 20. Battery pushing system: block diagram (Top), disassembled mechanical part (bottom left), geared micro-motor (bottom middle), completed system (bottom right)

4.4 Drawbacks and Improvements

The CISSbot hardware has now been implemented. Although the design is promising and it is able to function as we expect, there are some drawbacks in the technical details which we wish to improve in the future.

Mechanical stability:

To establish experiments quickly, plastics may feature as flexible materials. Although the CISSbot is assembled with several plastic pieces, the mechanical properties have not shown any unexpected errors to date. However, so far, there have been a few simple established experiments so we may need to conduct more complicated experiments to investigate the mechanical stability. In the near future, we may change plastics to aluminum materials to extend more functions to the CISSbot, e.g. a self-forming chain of robots, attaching each other to exchange batteries.

Electronics functions:

The compass provided unreliable angle measurement due to motion friction when the robot is moving. Actually, the compass acts as a passive sensor, and thus the magnetic field generated by two wheeled DC motors may effect it. Fortunately, we are currently using the sensor to sense only four bidirectional axes so that this is not serious problem. But it should be considered when the pre-built map is removed.

In the proximity mode, the infrared signal may interfere if two robots are too close. Moreover, the infrared signal sometimes jumps to an unexpected infrared receiver. As predicted, this may be a problem of signal strength, so we must pay attention to solving these shortcomings in the near future.

Control complexity:

As explained, the main goal of the CISSbot is to create truly autonomous robots through self-distributed energy. This is done by two methods, either coming back to a charging

station to refuel energy or exchanging energy with the other robots. However, these methods emphasize the techniques of motion planning in large populations. Given this assumption, the execution phases of a battery exchange process are a set of states (invisible state, visible state, close state, etc.), and every state must be successfully solved in order to ensure that the set of states ends completely. As a result, the success of the set leads to the success of a battery exchange. Although the current design obtains the full basic elements to control a battery exchange process between two CISSbots on a pre-built map, the new control algorithm still has to be improved in order to increase the percentage of successful battery exchange processes and save travel time.

Neighbor communications:

To perform a battery exchange process, a robot must first be driven to approach another robot side by side. Second, the two robots will have to use neighbor communication to negotiate with each other to find out the right battery boxes to be exchanged. Normally, a number of \sum_1^n neighbor communications has to be carried out to find the right battery boxes, and one more talk is needed to complete the process. However, wasteful communication time should not happen in large populations. Therefore, we have to pay more attention to this aspect in the future. A new method of battery exchange through direct attachment will soon be implemented to reduce, or even remove the number of neighbor communications soon.

General improvements:

The development of the CISSbots is long whiled with several constrained circumstances. For example, the battery choice would be able to lead to the size of the battery box, and the size of the battery box might decide the size of the robots and so on. Further, we might find it hard to produce aluminum pieces to make the robot, and thus the robot would essentially be assembled from numerous plastic pieces, which can make the robot slightly unstable if some hard tasks are required. The battery pushing mechanism could give us a trouble since there are many opinions about using a micro pneumatic air pump, shape memory alloys, or static-magnetic force but none have proved feasible after experimentation. Finally, the linear micromotor mechanism is an acceptable solution, although it is not perfect, due to some home-made parts.

In the near future, we have to pay more attention to interference in both neighbor communications and global broadcasting. This does not always happen, but it has sometimes made our robots to behave incorrectly. More investigation onto distance sensing capabilities, based on a smart beacon, would be preferable in order to remove the current grid-map.

5. Conclusion

We presented our study of randomized robot trophallaxis through the main aspects of modeling, simulation and real implementation. The modeling is kept at an abstract level in order to provide general analytical results of intergro-differential equation governing the evolution of expected energy levels and variance as function of position velocity and time. The model is partly used to evaluate the performance associated to embedded environments such as the position and density of charging station and robots. Ultimately, survivability is the final target of the developed model. Besides, the concept "randomized robot trophallaxis" is further clarified through simulation results. The developed simulation

showed that a group of mobile robots is able to be truly autonomous if and only if they are capable of "trophallaxis" containing self-refueling energy and self-sharing energy. To shed light on "randomized", several simulations were setup to examine in terms of density of robots, control algorithms, task allocation, and location of charging station. Finally, to increase the reality of our study, we consequently presented hardware implementation of the trophallatic robot. Details of mechanical architecture and modular electronics were described. Based on the implementation, we also pointed out the advantage and drawbacks of the current design and direction for future work.

6. Reference

Bettstetter. C, Hartenstein. H, and Perez-Costa.X (2002). Stochastic Properties of the Random Waypoint Mobility Model: Epoch Length, Direction Distribution, and Cell Change Rate. In *Proc. ACM Intern. Workshop on Modeling, Analysis, and Simulation of Wireless and Mobile Systems* (MSWiM), Atlanta, GA, USA, pp. 7-14, Sept 2002.

Le Boudec, Jean-Yves ; Vojnovic, Milan (2005). Perfect Simulation and Stationarity of a Class of Mobility Models, *IEEE INFOCOM* , Miami, 2005.

Øksendal, Bernt K. (2003). Stochastic Differential Equations: *An Introduction with Applications*. Springer, Berlin. ISBN 3-540-04758-1.

Camp. T, Boleng. J, and Davies. D, (2002) A survey of mobility models for ad hoc network research, *Wireless Communications and Mobile Computing*, vol. 2, no. 5, pp. 483-502, 2002.

Schiøler. S ; Martin Bøgsted. H.P. Schwefel (2005). Probabilistic Modelling of Information Propagation in Wireless Mobile Ad-Hoc Network. In *Proceedings of the International Symposium on Wireless Personal Multimedia Communications* (WPMC 2005). Aalborg : Center for TeleInFrastruktur (CTIF), Aalborg Universitet, 2005.

Medlock.J, Kot. K (2003). Spreading disease: Integro-differential equations old and new, *Mathematical Biosciences*, 184(2):201-222, 2003.

Moreno. Y, Nekovee. M, and Pacheco A.F. (2004) Dynamics of rumor spreading in complex networks, *Phys. Rev. E*. 69, 066130.

Camazine. S (1998), Protein Trophallaxis and the Regulation of Pollen Foraging by Honeybees, *Apidologie*, Vol.29, pp.113-126, 1998.

Sumpter. D.J.T and Beekman. M (2003), From Nonlinearity to Optimality: Pheromone Trail Forageing by Ants, *Animal Behaviour*, Vol. 66, pp.273-280.2003.

Payton. D, Estkowski. R, and Howard. H (2005), Robotics and The Logic of Virtual Pheromones, in *Swarm robotics, SAB 2004*. LNCS 3342, Springer Verlag, 2005, pp.45-57, 2005.

Ngo. T.D, Schiøler. H (2006), An approach to sociable robots through self-distributed energy, *In proceedings of the International Conferences on Intelligent Robots and Systems (IROS)"*, Beijing, 2006.

Ieropoulos. I, Melhuish. C, Greenman. J (2004), Energetically autonomous robots, in *Proceedings of the 8th Intelligent Autonomous System Conferences (IAS-8)*, Amsterdam, The Netherlands, pages 128-135, 2004.

Ngo. T.D, Raposo. H, H. Schiøler (2007), Multi-agent robotics: towards energy autonomy, in *Proceedings of International Conference in Artificial Life and Robotics (AROB'12th)*, Beppu, Oita, Japan, 2007.

Ieropoulos. I, Melhuish. C, Greenman. J, Horsfield. I (2005), EcoBotII: An artificial agent with a natural metabolism, *International Journal of Advanced Robotic Systems*, Vol2, 2005.

Mei. Y, Lu. Y.H, Charlie Hu. Y, and George Lee C. S. (2006a), Deployment of Mobile Robots with Energy and Timing Constraints, *IEEE Transactions on Robotics*, 2006.

Mei. Y, Lu. Y.H, Charlie Hu. Y, and George Lee C. S. (2006b), Energy-Efficient Mobile Robot Exploration, *IEEE International Conference on Robotics and Automation*, USA, 2006.

Murata. H, Yoshida. E, Tomita. K, Kurokawa. H, Kamimura. A, and Kokaji. S (2000), Hardware design for modular robotic system, *In proceedings of the International Conferences on Intelligent Robots and Systems (IROS)*, pages 2210-22127, 2000

Lund. H. H., Beck. H. H., Dalgaard. L, Self-Reconfigurable Robots with ATRON Modules (2005), In *Proceedings of 3rd International Symposium on Autonomous Mini-robots for Research and Edutainment (AMiRE 2005)*, Springer-Verlag, Fukui, 2005.

Yoshida. E, Murata. H, Mamimura. A, Tomita. K, Kurokawa. H, and Kokaji. S (2001), A motion planning method for a self-reconfigurable modular robot, In *proceedings of the International Conferences on Intelligent Robots and Systems (IROS)*, pages 1049-1054, 2001.

Groß. R, Bonani. M., Mondada F., Dorigo M. In K. Murase, K. Sekiyama, N. Kubota, T. Naniwa (2005), and J. Sitte, editors, Autonomous Self-assembly in a Swarm-bot, Proc. of the 3rd Int. Symp. on Autonomous Mini-robots for Research and Edutainment, AMiRE 2005, pages 314-322. Springer Verlag, Berlin, 2006.

Ostergaard. E. H and Lund. H.H, (2004), Distributed Cluster Walk for the ATRON Self-Reconfigurable Robot, In *Proceedings of the The 8th Conference on Intelligent Autonomous Systems (IAS-8)*, Amsterdam, Holland, Pages 291-298, March 10-13, 2004

Dorigo M., Tuci E., Trianni V., Groß R., Nouyan S., Ampatzis C., Labella T.H., O'Grady R., Bonani M., Mondada F (2006), SWARM-BOT: Design and Implementation of Colonies of Self-assembling Robots, *Computational Intelligence: Principles and Practice*, Gary Y. Yen and David B. Fogel (eds.), IEEE Computational Intelligence Society, NY, 2006, 103-135.

Mondada F., Gambardella L.M., Floreano D., Nolfi S., Deneubourg J.-L., Dorigo M, (2005) SWARM-BOTS: Physical Interactions in Collective Robotics, *IEEE Robotics & Automation Magazine*, vol. 12, june 2005, pp. 21-28.

O'Grady R., Groß R., Mondada F., Bonani M., Dorigo M. (2004) In M.S. Capcarrere and A.A. Freitas and P.J. Bentley and C.G. Johnson and J. Timmis, editors, Self-assembly on demand in a group of physical autonomous mobile robots navigating rough terrain, *Advances in Artificial Life, Proceedings of the 8th European Conference on Artificial Life*, pages 272-281, Springer-Verlag.



Recent Advances in Multi Robot Systems

Edited by Aleksandar Lazinica

ISBN 978-3-902613-24-0

Hard cover, 326 pages

Publisher I-Tech Education and Publishing

Published online 01, May, 2008

Published in print edition May, 2008

To design a team of robots which is able to perform given tasks is a great concern of many members of robotics community. There are many problems left to be solved in order to have the fully functional robot team. Robotics community is trying hard to solve such problems (navigation, task allocation, communication, adaptation, control, ...). This book represents the contributions of the top researchers in this field and will serve as a valuable tool for professionals in this interdisciplinary field. It is focused on the challenging issues of team architectures, vehicle learning and adaptation, heterogeneous group control and cooperation, task selection, dynamic autonomy, mixed initiative, and human and robot team interaction. The book consists of 16 chapters introducing both basic research and advanced developments. Topics covered include kinematics, dynamic analysis, accuracy, optimization design, modelling, simulation and control of multi robot systems.

How to reference

In order to correctly reference this scholarly work, feel free to copy and paste the following:

Trung Dung Ngo and Henrik Schioler (2008). Randomized Robot Tropheallaxis, Recent Advances in Multi Robot Systems, Aleksandar Lazinica (Ed.), ISBN: 978-3-902613-24-0, InTech, Available from: http://www.intechopen.com/books/recent_advances_in_multi_robot_systems/randomized_robot_trophallaxis



InTech Europe

University Campus STeP Ri
Slavka Krautzeka 83/A
51000 Rijeka, Croatia
Phone: +385 (51) 770 447
Fax: +385 (51) 686 166
www.intechopen.com

InTech China

Unit 405, Office Block, Hotel Equatorial Shanghai
No.65, Yan An Road (West), Shanghai, 200040, China
中国上海市延安西路65号上海国际贵都大饭店办公楼405单元
Phone: +86-21-62489820
Fax: +86-21-62489821